*Current Research (2017) Newfoundland and Labrador Department of Natural Resources Geological Survey, Report 17-1, pages 19-39*

# LITHOGEOCHEMISTRY OF MAFIC INTRUSIVE ROCKS FROM THE BONAVISTA PENINSULA, AVALON TERRANE, NORTHEASTERN NEWFOUNDLAND

A.J. Mills and H.A.I. Sandeman[1]
Regional Geology Section
[1]Mineral Deposits Section

## ABSTRACT

*Lithogeochemical results are presented for 52 samples of mafic intrusive rocks from the Avalon Terrane on the Bonavista Peninsula. Plagioclase porphyritic gabbro dykes (Type 1) occur west of the Plate Cove volcanic belt and cut marine flysch of the* ca. *620–605 Ma Connecting Point Group in the Sweet Bay area. These are evolved, calk-alkaline basalts that have well-developed negative HFSE anomalies and show evidence for high degrees of lithospheric recycling associated with their formation. Type-2 gabbro dykes also occur west of the Plate Cove volcanic belt and are transitional to (weakly) calc-alkaline basalts having variable Th/Nb and La/Nb relationships and are interpreted to be derived from a lithosphere-contaminated, slightly enriched (E-MORB) shallow-mantle source. Type-3 gabbro dykes are similar to Type 2, but have smaller negative Nb anomalies and are inferred to be younger based on their spatial restriction to the <600 Ma Musgravetown Group, which includes the east-facing Plate Cove volcanic belt and overlying Neoproterozoic siliciclastic sequences of the proximal Rocky Harbour and distal Big Head formations. Type-4 dykes occur on the southeast part of the peninsula, near British Harbour, and cut mainly proximally derived, epiclastic rocks of the Musgravetown Group. These are slightly alkaline and have relatively low Th/Nb ratios, indicating that crustal contamination was not important in their petrogenesis. Type-5 gabbro dykes, the youngest, are post-Cambrian, have alkaline basalt compositions and ocean-island basalt-like chemistry, and a minor lithospheric input as indicated by supra-asthenospheric Th/Nb values.*

*Recent U–Pb (zircon) results constrain the timing of magmatism. Type-1 dykes appear to be petrologically linked to the* ca. *600 Ma Headland basalts (lower Bull Arm Formation) that unconformably overlie the thrust-stacked, shoaling-upward turbiditic rocks of the Connecting Point Group. Type-2 and 3 dykes may be petrogenetically linked to the two previously recognized mafic series of the fault-bounded, mainly subaerial Plate Cove volcanic belt. Type-2 dykes resemble the earlier,* ca. *592 Ma Plate Cove volcanic belt series, whereas <579 Ma Type-3 dykes are more similar to the younger Plate Cove volcanic belt series derived from shallower, more enriched asthenospheric mantle. Timing of intrusion of the alkalic Type-4 dykes is loosely constrained as post-579 Ma and pre-565 Ma, based on petrological trends and structural relationships. Type-5 dykes are post-Cambrian, as they crosscut Cambrian strata.*

## INTRODUCTION

Few petrological and lithogeochemical studies have been conducted on rocks of the northwestern Avalon Terrane (*e.g.*, Malpas, 1971; Hussey, 1979), and these studies preceded the advent of modern methods that facilitate the precise determination of abundances of critically important incompatible trace elements. Modern geochemistry analytical methods and improved detection limits, combined with new petrological interpretation, have led to a more refined understanding of petrology in known tectonic settings (*e.g.*, Longerich *et al.*, 1990; Pearce, 1996), and this has been applied by Mills and Sandeman (2015) in the investigation of the mafic volcanic rocks of the Bonavista Peninsula. The rocks investigated by Mills and Sandeman (2015) include: 1) glomerocrystic basalts and basaltic andesites exposed on the northern tips of three prominent headlands in the Sweet Bay area (Headland basalt: HB); 2) two volcanic series within the north-trending, east-dipping Plate Cove volcanic belt (PCvb1 and PCvb2), and; 3) the Dam Pond basalts (DP), which outcrop around a small pond midway between Upper Amherst Cove and Catalina. Each of these three, spatially defined volcanic packages has distinct lithogeochemistry, reflecting differing tectonic settings. The HB are plagioclase porphyritic to glomerocrystic, calc-alkaline basalts enriched in large ion lithophile elements (LILE) and light

rare-earth elements (LREE), consistent with formation in a mature continental subduction setting. Basalts of the Plate Cove volcanic belt (PCvb) are commonly aphanitic, but locally have well-developed sieve-textured plagioclase phenocrysts interpreted to result from resorption and dissolution. They have transitional geochemical signatures (arc-like to E-MORB-like), and are derived from a lithosphere-contaminated, slightly enriched, shallow-mantle, mid-ocean ridge basalt (E-MORB) source. The DP basalts are alkaline, lack plagioclase phenocrysts, and possess distinct ocean island basalt (OIB)-like chemistry and evidence of a minor lithospheric contribution.

This paper builds upon the previous petrological investigations through petrogenetic study of the mafic dykes that crosscut the rocks of the Bonavista Peninsula. Type-1 (n=13) and Type-2 (n=20) dykes are the most common. They occur west of the PCvb and cut marine flysch of the ca. 620–605 Ma Connecting Point Group (Mills *et al.*, 2016b) in the Sweet Bay area. Type-3 dykes (n=11) occur on the east side of the east-facing PCvb and cut rocks of the <600 Ma Musgravetown Group. Type-4 dykes (n=5) appear to be restricted to the southwest part of the Bonavista Peninsula, mainly in the vicinity of British Harbour (Figure 1). Type 5 (n=2), the least common dyke type, is currently only recognized west of the PCvb, and at one location the dyke crosscuts black shale of the Manuels Formation of the Cambrian Harcourt Group.

## REGIONAL GEOLOGY

The Bonavista Peninsula, part of the Avalon Terrane of Newfoundland, is primarily composed of Neoproterozoic siliciclastic and volcaniclastic rocks of the Connecting Point and Musgravetown groups (CPG and MG, respectively). The CPG is part of an extensive marine basin that formed adjacent to an active volcanic arc, remnants of which are preserved in the underlying, mainly volcanic *ca.* 620 Ma Love Cove Group, outcropping to the west of the study area in the vicinity of Clode Sound at Terra Nova National Park (Widmer, 1949; Knight and O'Brien, 1988; O'Brien *et al.*, 1989; Dec *et al.*, 1992). The MG is a thick succession of red and green, mainly coarse-grained clastic rocks and basal volcanic rocks that overlie the CPG, and is, in turn, overlain by the quartz arenite-dominated, marginal marine, Cambrian Random Formation (Hayes, 1948; Smith and Hiscott, 1984). On the Bonavista Peninsula, the MG is subdivided into the following formations (in ascending order): the Cannings Cove Formation, a dominantly red basal conglomerate unit (not shown on Figure 1); the Bull Arm Formation (BAF), a mainly terrestrial volcanic succession; the Rocky Harbour Formation, composed mainly of shallow-marine, coarse-grained siliciclastic rocks and; the Crown Hill Formation, composed of terrestrial red beds (Jenness, 1963) (Figure 1). Recently, grey siltstone, which apparently interfingers coarser grained, more proximally derived rocks conventionally assigned to Rocky Harbour Formation, has been assigned to the Big Head Formation (Normore, 2010; Figure 1), a lithologically similar MG formation that overlies BAF rocks in the Placentia Bay area (McCartney, 1967). A lower Paleozoic transgressive marine succession, the base of which is delineated by the Random Formation, unconformably overlies the CPG in the southern Sweet Bay area (Mills, 2014; Mills *et al.*, 2016a) and conformably to disconformably overlies the top of the MG in the Keels area (Figure 1). The Conception–St. John's–Signal Hill groups outcrop throughout the area east of the Spillars Cove–English Harbour Fault Zone (SCFZ, Figure 1; O'Brien and King, 2002).

# FIELD AND PETROGRAPHIC DESCRIPTIONS

## TYPE-1 DYKES

Twelve samples were collected from eleven dykes that are classified as Type-1; their distribution is shown in Figure 1. These are coarse-grained dykes, typically 1−3 m thick, and were termed either gabbro dykes or plagioclase-phyric basalt dykes in the field (*e.g.*, Plate 1A, B). Orientations were determined for six of these (Table 1): three trend north-northwest (347–352°), two northeast (30 and 45°), and one southeast (140°). The dykes are all steeply dipping and, as for all orientation data referred to herein, the trend reflects the dip direction determined by the right hand rule convention. Three variants have been identified through field and petrographic analyses. Subtype A is composed of clinopyroxene-phyric basalt (n=4); subtype B is composed of plagioclase-phyric basalt (n=5) and; subtype C is composed of gabbro (n=3). Subtype A contains up to 30%, fresh, euhedral clinopyroxene phenocrysts (≤5 mm) set in a very fine-grained, pilotaxitic groundmass (Plate 1C). Plagioclase occurs as slightly saussuritized, <200 μm laths in the groundmass. Subtype B contains plagioclase phenocrysts, locally sieve-textured and up to 5 mm in length, occurring in a fine-grained, trachytic plagioclase-rich groundmass (Plate 1D). Subtype C, gabbro dykes, contain >1 mm crystals of clinopyroxene and plagioclase, and minor intersertal material (Plate 1E). Plagioclase in the gabbro dykes is commonly saussuritized and rare sieve-textured phenocrysts are also present. A thin section from a contact between subtype A and B dykes preserves sub-millimetre bayonet-like apophysis of the former that cuts the latter, (Plate 1F), indicating that emplacement of the clinopyroxene-phyric dykes postdates the intrusion of at least some of the basalt dykes.

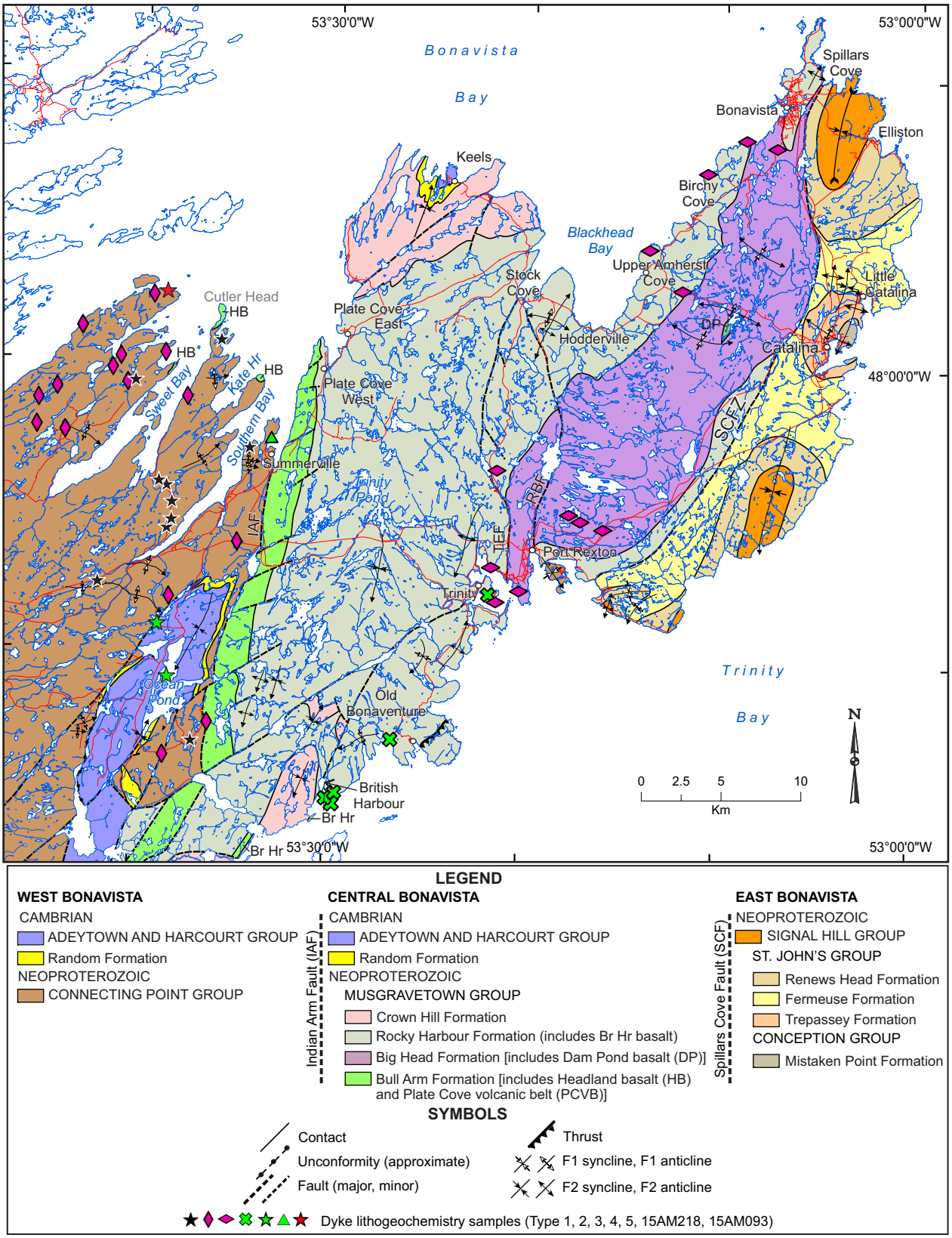


**LEGEND**

**WEST BONAVISTA**
- CAMBRIAN
- ADEYTOWN AND HARCOURT GROUP
- Random Formation
- NEOPROTEROZOIC
- CONNECTING POINT GROUP

**CENTRAL BONAVISTA**

Indian Arm Fault (IAF)
- CAMBRIAN
- ADEYTOWN AND HARCOURT GROUP
- Random Formation
- NEOPROTEROZOIC
- MUSGRAVETOWN GROUP
- Crown Hill Formation
- Rocky Harbour Formation (includes Br Hr basalt)
- Big Head Formation [includes Dam Pond basalt (DP)]
- Bull Arm Formation [includes Headland basalt (HB) and Plate Cove volcanic belt (PCVB)]

**EAST BONAVISTA**

Spillars Cove Fault (SCF)
- NEOPROTEROZOIC
- SIGNAL HILL GROUP
- ST. JOHN'S GROUP
- Renews Head Formation
- Fermeuse Formation
- Trepassey Formation
- CONCEPTION GROUP
- Mistaken Point Formation

**SYMBOLS**
- Contact
- Unconformity (approximate)
- Fault (major, minor)
- Thrust
- F1 syncline, F1 anticline
- F2 syncline, F2 anticline
- Dyke lithogeochemistry samples (Type 1, 2, 3, 4, 5, 15AM218, 15AM093)

**Figure 1.** *Simplified geology map of the Bonavista Peninsula showing the distribution of dykes sampled for lithogeochemistry (modified from O'Brien and King, 2005). Abbreviations: HB – Headland basalt; DP – Dam Pond basalt; IAF – Indian Arm fault; RBF – Robinhood Bay fault; TEF – Trinity East fault; Br Hr – British Harbour basalt; SCFZ – Spillars Cove fault zone.*

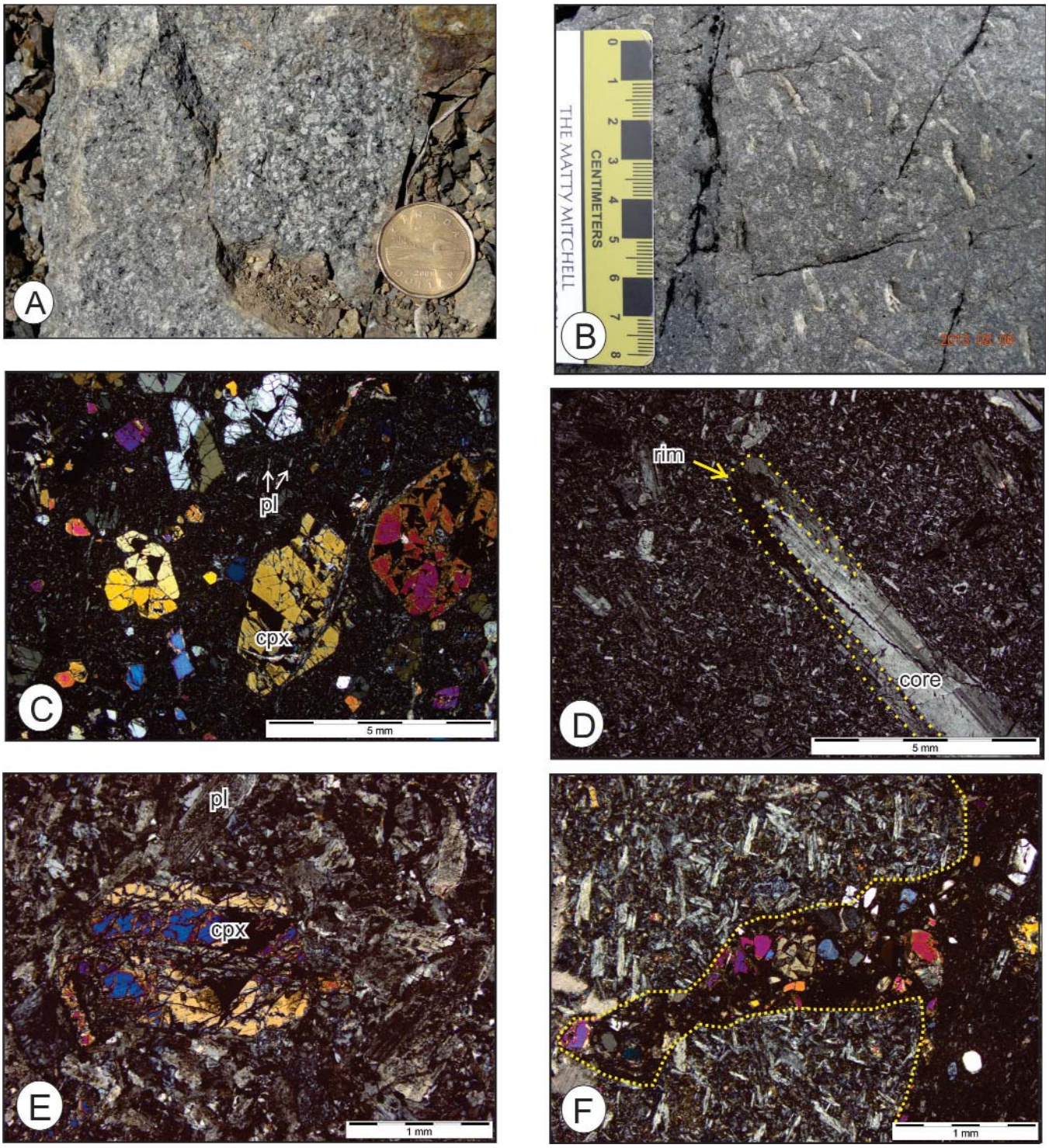


**Plate 1.** *Type-1 dykes. A) Gabbro dyke (sample 13AM156B) from Sweet Bay area; Canadian $1 coin for scale is approximately 2.6 cm in diameter; B) Plagioclase-phyric dyke (sample 13AM319B) showing flow alignment of plagioclase phenocrysts, Sweet Bay area; compositional zoning is indicated in the plagioclase phenocrysts by the presence of thin (up to 1 mm), bright rims surrounding lighter grey cores; C) Subhedral clinopyroxene phenocrysts in a very fine-grained, pilotaxitic groundmass of a clinopyroxene-phyric basalt dyke (sample 13AM152B); D) Zoned plagioclase phenocryst enveloped by weakly developed trachytic/flow texture (sample 13AM319B); E) Anhedral clinopyroxene crystal in Type-1 gabbro dyke (sample 13AM156B); F) Bayonet-like apophasis of clinopyroxene-phyric basalt in a trachytic-textured dyke. Abbreviations: pl – plagioclase; cpx – clinopyroxene.*

**Table 1.** Salient field, petrographic and geochemical features of the five types of dykes identified on the Bonavista Peninsula. Mineral abbreviations (Pl, Cpx, Chl) as per Kretz (1983); Eu* is the square root of the product of chondrite-normalized Sm and Gd values [$Eu^*=\sqrt{(SmCN*Gd_{CN})}$], as per Taylor and McLennan (1985); CN subscript denotes chondrite-normalized ratios

| Dyke Type | Total # Dykes | Dominant Trend | Minor Trend | Distinguishing Petrographic Features | Mg# | $(La/Yb)_{CN}$ | $(La/Sm)_{CN}$ | $(Gd/Yb)_{CN}$ | Eu/Eu* | $(Th/La)_{CN}$ | $(La/Nb)_{CN}$ | $(Th/Nb)_{CN}$ |
|---|---|---|---|---|---|---|---|---|---|---|---|---|
| 1 | 11 | NNW (3) | NE (2)<br>SE (1) | Cpx-phyric subset A (most primitive); Pl-phyric subset B; Gabbro subset C | 54.2 | 7.07 | 2.63 | 1.97 | 0.86 | 1.98 | 3.86 | 2.93 |
| 2 | 16 | NE (4) | E (3); S (2) | Subophitic; sieve-textured pl; amygdales rare | 40.9 | 3.59 | 1.54 | 1.84 | 1.00 | 0.68 | 2.22 | 1.51 |
| 3 | 11 | W (6) | NW (2);<br>NNE (1) | Intergranular texture; rare relict cpx; common chl ± carb amygdales | 36.0 | 3.21 | 1.55 | 1.68 | 1.02 | 0.84 | 1.28 | 1.10 |
| 4 | 5 | NW (2) | N-S (2) | Pilotaxitic; minor pl phenocrysts | 32.3 | 6.91 | 2.43 | 1.80 | 0.92 | 0.69 | 1.11 | 0.74 |
| 5 | 2 | NNE (1) | | Ophitic cpx-pl (1); trachytic with possible cpx or ol pseudomorphs (1) | 53.8 | 8.18 | 2.74 | 2.17 | 1.00 | 1.04 | 0.93 | 0.98 |

## TYPE-2 DYKES

Twenty samples from 16 dykes are grouped as Type-2; four samples are duplicates. The dykes range from 0.4–10 m thick and orientation data was obtained for nine (Table 1). Four are northeast-trending (045–065°), three are east-trending (080–095°) and two are south-trending (180–200º). All east- and northeast-trending dykes are gabbroic in composition. Of the south-trending dykes, one is gabbroic and has straight margins and no apparent chill zone (Plate 2A), whereas the other is basaltic and has an apophasis and cuspate contact margins with the host sedimentary rocks, consistent with synsedimentary emplacement (Plate 2B).

Most (n=12) of the dykes are gabbroic and display intergranular plagioclase and clinopyroxene, having minor intersertal glass variably altered to chlorite, as well as Fe-oxides (magnetite ± ilmenite) commonly rimmed by titanite (Plate 2C). Trace pyrite, pyrrhotite and chalcopyrite were noted in some of the Type-2 gabbro dykes. Three gabbro dykes have chlorite amygdales, whereas sieve-textured plagioclase phenocrysts, ranging up to 1 mm diameter, were only noted in one Type-2 gabbro dyke.

A small subset of Type-2 dykes are plagioclase-phyric basalts (n=4). These typically have either sieve-textured plagioclase phenocryst cores (Plate 2D) or heavily saussuritized cores that have relatively unaltered rims. The groundmass is composed of plagioclase laths showing well-developed trachytic texture, minor intergranular brownish clinopyroxene (titano-augite?), and sub-mm chlorite amygdales.

## TYPE-3 DYKES

Eleven samples of Type-3 dykes were collected, and orientation data were determined for nine dykes (Table 1); these range in thickness from 1 to approximately 20 m. Six are roughly west-trending (245–290°), two are northwest-trending (330 and 345°), and one trends north-northeast (012°). At least one of the dykes is oriented parallel to a well-developed cleavage in the MG host rocks (Plate 3A), and this structural weakness may have provided a conduit for magma emplacement.

The dykes typically preserve intergranular gabbroic texture, with the exception of one very fine-grained basaltic example. The dykes generally display an intergranular texture, having up to 15% variably preserved relict clinopyroxene, 60–75% subhedral, variably altered plagioclase, 5–10% opaque minerals (mainly magnetite), and minor interstitial chlorite and titanite. Minor patchy chlorite ± carbonate alteration locally occurs in some dykes. Biotite + epidote are abundant in one sample and are interpreted to be secondary

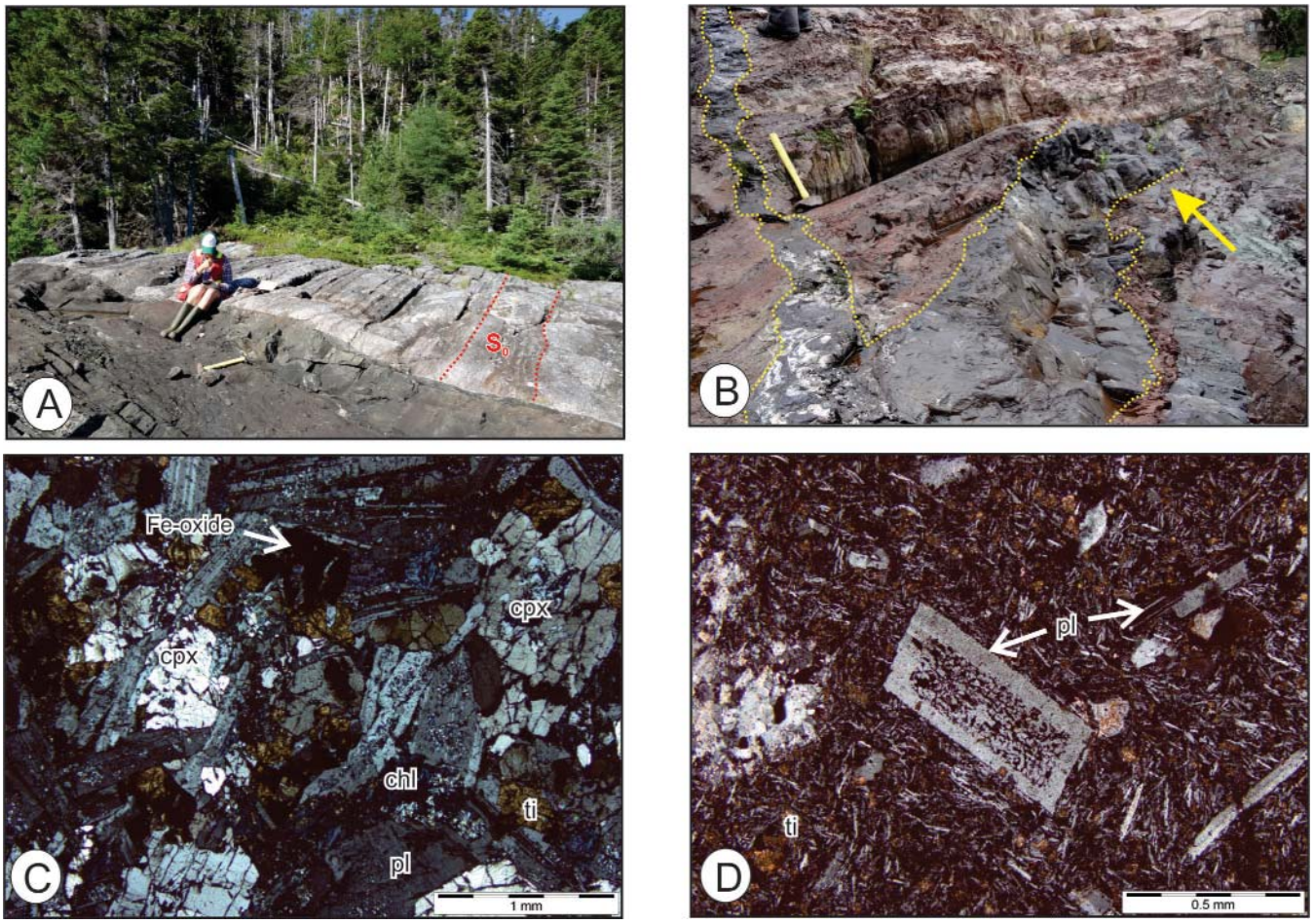


**Plate 2.** *A) South-trending (180/50°) Type-2 gabbro dyke with straight margins crosscuts turbidites of the Connecting Point Group at a high angle to bedding ($S_0$); view to the southwest; B) Type-2 basaltic dyke (sample 13AM160B) displaying bifurcation with one arm (left side in photograph) cutting bedding at a high angle whereas the other (to the right) cuts bedding at a low angle, becoming subparallel to bedding (yellow arrow). Note the cuspate margins of the left arm (near hammer) consistent with intrusion of the dyke into soft sediment before compaction and lithification of the host sandstone. Dyke trend is ~200°; view to the south-southwest; hammer is ~40 cm long; C) Type-2 gabbro dyke is composed of inter-granular plagioclase and clinopyroxene; note minor chlorite (replacing intersertal glass) and iron oxide rimmed by titanite; viewed under cross-polarized light; D) Zoned plagioclase phenocryst with a sieve-textured core and subhedral, fresh mantle; viewed under cross-polarized light. Abbreviations: pl – plagioclase; cpx – clinopyroxene; ti – titanite; chl – chlorite.*

phases. Poorly preserved, sieve-textured feldspar was noted in one Type-3 gabbro dyke (Plate 3B).

## TYPE-4 DYKES

Five dykes are designated as Type-4, and orientation data was determined for four of these. Two are northwest-trending (300°), whereas the other two are north-, and south-trending, respectively (350° and 185°). The south-trending dyke (Sample 14AM286A) is a basalt, approximately 10 m thick, and displays well-developed columnar jointing (Plate 4A). The two northwest-trending dykes are gabbroic, variably altered to chlorite and carbonate, and petrographically resemble the Type-3 gabbro dykes (Plates 3B and 4B). One Type-4 dyke is a plagioclase-phyric andesite (orientation not available; Plate 4C) and is chemically identical to the north-trending, 1.5-m-thick dyke (Plate 4D; *see* below).

## TYPE-5 DYKES

Based on their chemical composition (*see* below), two dykes are classified as Type-5. One is a 10-m-thick gabbro that trends 015°, and crosscuts black shale of the Manuals Formation (Harcourt Group; Figure 1). This dyke displays a well-developed ophitic texture and has well-preserved, subhedral, clinopyroxene and plagioclase crystals up to 1 mm. Minor iron-oxide minerals are rimmed by titanite (Plate 5A). The dyke's margins are not exposed at the sample location, so crosscutting relationships with Acadian, $D_2$ deformation, were not observed. It is also unclear if the dyke

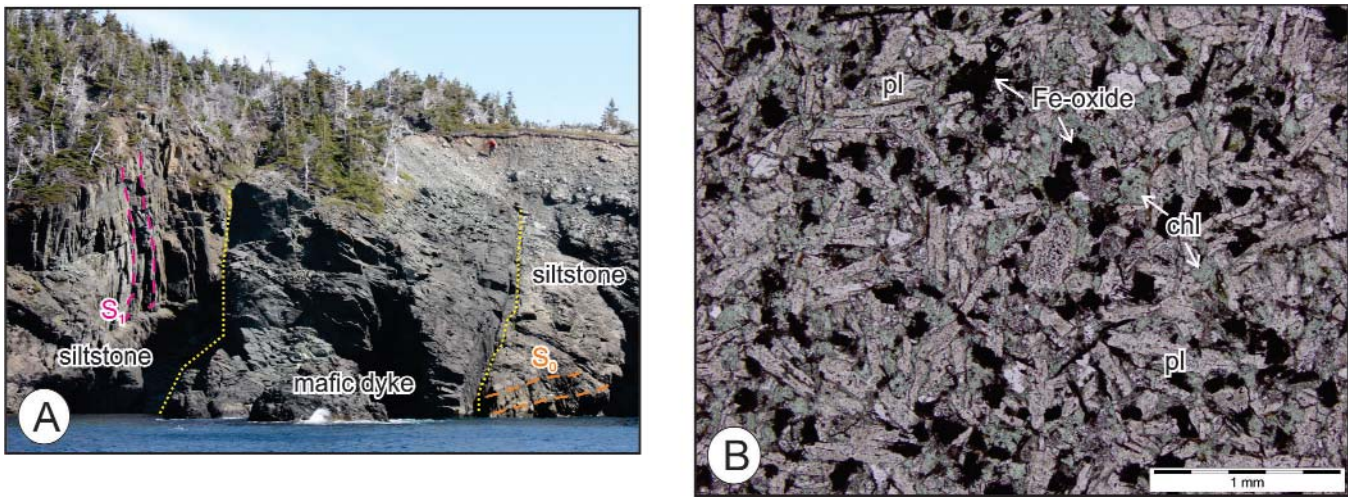


**Plate 3.** *A) View to the southeast of a northwest-trending, Type-3 dyke exposed on the shoreline of Blackhead Bay, 800 m west of Middle Amherst Cove (sample 09LN095A). Note that the sub-vertical cleavage (red dashed line) developed in the shallowly dipping sedimentary rocks on the northeast side of the dyke appears to be subparallel to the dyke margins; B) Photomicrograph of a typical Type-3 dyke (sample 15AM141), from the west side of the Skerwink Peninsula on Trinity Bay, showing 1-mm plagioclase laths, interstitial chlorite (likely replacing intersertal glass), ~10% opaque minerals and a sieve-textured feldspar (centre); viewed under plane-polarized light. Abbreviations: pl – plagioclase; chl – chlorite.*

crosscuts $S_2$ cleavage at map scale, as its north-northeast-trending orientation is parallel to the dominant trend of $D_2$ structural features in the study area. The second Type-5 dyke, for which the orientation and thickness could not be determined, is a highly altered phenocrystic basalt and contains possible clinopyroxene or olivine pseudomorphs (now prehnite?) in a carbonate-altered, trachytic-textured groundmass (Plate 5B). Minor rutile and hematite are also present.

## PETROCHEMISTRY

### ANALYTICAL METHODS

This lithogeochemical study aims to characterize the compositional variations of mafic intrusive rocks and to provide insight into their origin. Representative samples devoid of weathering, and free of veins and fractures were collected for analysis. Samples were analyzed at the Geochemical Laboratory, Department of Natural Resources, Government of Newfoundland and Labrador, for their major-, and select trace-element contents according to the method outlined in Finch (1998) and Mills and Sandeman (2015). A total of 52 samples of mafic intrusive rocks were analyzed, and one representative sample of each of the Type-1, -2, -3 and -4 dykes, and both samples of Type-5 dykes are presented in Table 2. Rock samples were collected by the lead author (AM prefix) or by L. Normore (09LN and 10LN prefixes). The complete dataset will be released as a Geological Survey of Newfoundland Open File.

## ROCK CLASSIFICATION

Conventional major- and mobile trace-element classification plots may lead to spurious interpretations when applied to altered igneous rocks (*e.g.*, Middleburg *et al.*, 1988; Ross and Bédard, 2009). Mills and Sandeman (2015) demonstrated that alteration has affected many of the major and mobile trace elements in the volcanic rocks of the Bonavista Peninsula, and therefore lithogeochemical interpretations of the Bonavista intrusive rocks are based upon the relatively immobile trace elements, including the high-field-strength elements (HFSEs) and the rare-earth elements (REEs).

Based upon commonly used rock classification diagrams [*e.g.*, total alkali *vs.* silica diagram of Lebas *et al.* (1986) and the $Zr/TiO_2$ *vs.* Nb/Y discrimination diagram of Pearce (1996)], Type-1 dykes are classified as basalts and basaltic andesites, Type-2 and Type-3 dykes are classified as basalts, and Type-4 and Type-5 dykes are typically classified as alkali basalts, with the exception of one Type-4 dyke that is a trachyte, and one unusual dyke, a petrogenetic outlier in the dataset, that is dacitic in composition (Figure 2A, B). When plotted on the Th/Yb *vs.* Zr/Y discrimation diagram of Ross and Bédard (2009), Type-1 dykes are classified as being calc-alkaline, whereas Type-2 and Type-3 dykes are classified as being transitional between calc-alkaline and tholeiitic basalts (Figure 2).

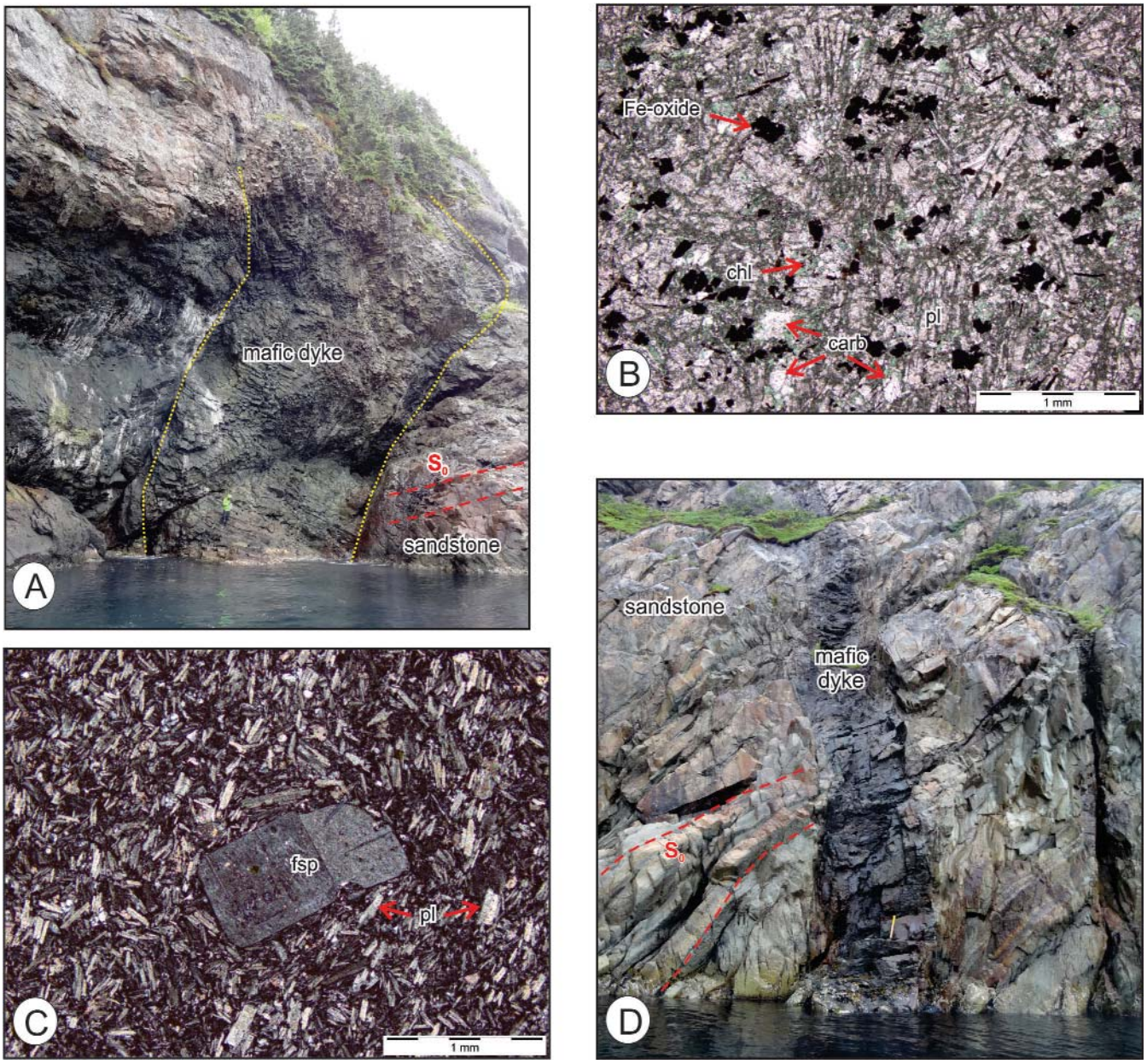


**Plate 4.** *A) Columnar-jointed, south-trending, 10-m-thick Type-4 basalt dyke (sample 14AM286A); viewed to the north; geologist is approximately 1.8 m tall; B) Photomicrograph of Type-4 gabbro dyke sample 14AM299C, showing saussuritized plagioclase laths, interstitial chlorite, opaques and patchy carbonate alteration (bright white), taken under plane-polarized light; C) Photomicrograph of plagioclase-phyric andesite dyke (sample 10LN727C) showing a subhedral feldspar phenocryst in a trachytic-textured groundmass; viewed under cross-polarized light; D) View to the north of 1.5-m-thick aphanitic, Type-4 mafic dyke (sample 14AM287B). Abbreviations: pl – plagioclase; chl – chlorite; carb – carbonate; fsp – feldspar.*

## MAJOR- AND TRACE-ELEMENT GEOCHEMISTRY

Most samples (all types of dykes) have low to moderate magnesium numbers (Mg#; 21–55). Type-1 and Type-5 dykes have the highest Mg#, Cr and Ni contents (Table 2). The most primitive of the Type-1 dykes have high Mg#s (up to 73), Cr (up to 956 ppm) and Ni (up to 178 ppm) abundances. Type-2 dykes have moderate Mg#s, Cr and Ni, whereas Type-3 and -4 have the lowest Mg#s, Cr and Ni.

On bivariate plots, all dyke types show a trend of decreasing Mg# and increasing Zr with fractionation (Figure 3I). Positive correlations are evident between the compatible transition elements (*e.g.*, Cr, V and Ni) and Mg# (Figure 3A,

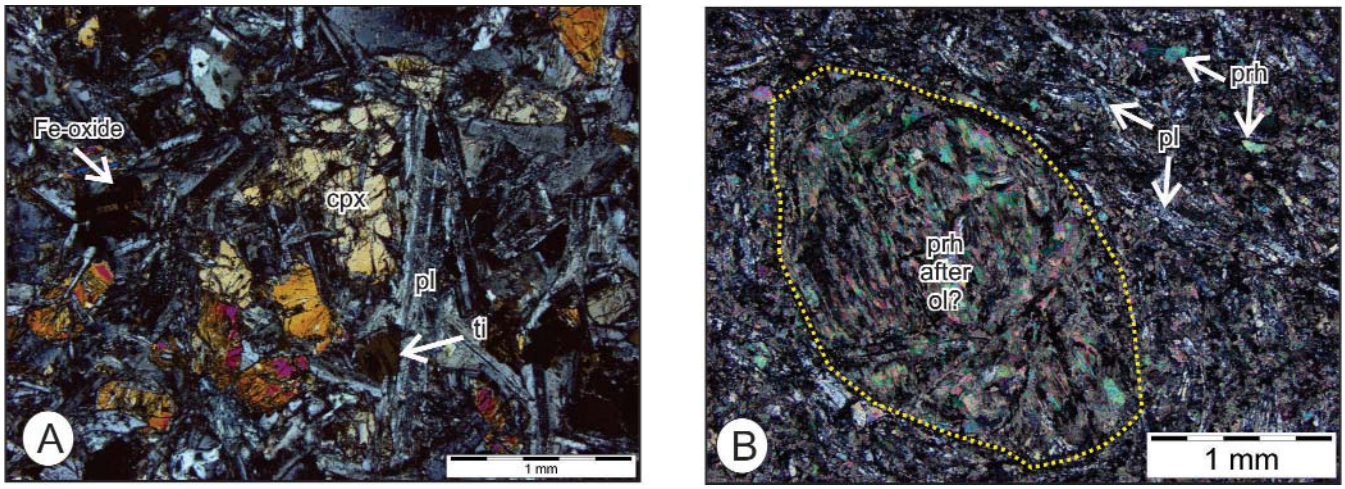


**Plate 5.** *Photomicrographs of Type-5 dyke. A) Sample 13AM279A which crosscuts black shale of the Manuels River Formation (Harcourt Group) at Ocean Pond in the Sweet Bay area. It consists of unaltered clinopyroxene and plagioclase having well-developed ophitic texture, and minor iron oxides commonly rimmed by titanite; B) Altered basalt dyke (sample 13AM057C), which is located proximal to a northeast-trending fault that separates the CPG to the west, from Paleozoic rocks to the east. The rock contains pseudomorphs of clinopyroxene or possibly olivine, replaced by prehnite (?), talc, carbonate and white mica possibly surrounded by altered plagioclase laths that preserve rapid cooling textures. Abbreviations: pl – plagioclae; cpx – clinopyroxene; ti – titanite; ol – olivine; prh – prehnite.*

D, E), whereas variably negative correlations are noted between most incompatible elements and Mg# (*e.g.*, Ti, P, Th, Yb). Positive linear correlation is evident between most of the highly incompatible elements, as illustrated by the $TiO_2$ *vs.* Zr, Th *vs.* Zr, and Y *vs.* Zr plots (Figure 3J–L). Petrochemical trends, observed using Mg#, are most evident in the data for Type-1 dykes (Figure 3), as these have the greatest range in Mg#. Similar trends are evident in Type-2 and -3 dykes, albeit less obvious because of their smaller range in Mg#. Substantial overlap exists between the fields defined by the Type-2 and -3 dykes. Type-4 and -5 basalt dykes show apparent complexity, but comprise too few samples (n=5, n=2, respectively) to define petrological trends.

In terms of alkalinity, Type-1 dykes are clearly calc-alkaline as evidenced by their high Th content, 'horizontal', low abundance $TiO_2$ trends with respect to Y/Nb, and enrichment of La relative to Nb and Y (Figure 4A–D). None of the Bonavista dyke types examined herein are clearly N-MORB tholeiites (Figure 2A, C). Dyke Type-2 and -3 are petrochemically similar and display partial overlap on most discrimination diagrams (Figure 4). On the Wood (1980) discrimination plot (Figure 4A), Type-2 and -3 dykes are transitional between E-MORB and calc-alkaline fields. On the Cabanis and Lecolle (1989) discrimination plot, Type-2 dykes overlap the calc-alkaline and continental fields, owing to their moderate La enrichment, whereas Type-3 dykes plot mainly within the continental field (Figure 4C). The wide range of Y/Nb ratios (Figure 4B) and strong $FeO^T$ and $TiO_2$ enrichment in Type 2 and 3 dykes is consistent with trends exhibited by many continental tholeiites (Floyd and Winchester, 1975; Murphy *et al.*, 1990). Type-2 dykes generally have higher Y/Nb ratios than Type-3 dykes (Figure 4B) and higher La/Nb ratios (Figure 4D). On the Zr/Y *vs.* Zr plot of Pearce (1983), all dyke samples from the Bonavista Peninsula, with the exception of one outlier, plot in the continental-arc field (Figure 4E).

The more alkali basalts of Type-4 and -5 dykes plot in the E-MORB and OIB fields of Wood (1980; Figure 4A), respectively, and relatively low in the continental field of Cabanis and Lecolle (1989); Type-5 overlaps the alkaline/continental rift field (Figure 4C). Type-4 and -5 also exhibit steep $TiO_2$ trends with respect to Y/Nb, owing to low variation in Y/Nb (Figure 4B). Type-4 dykes could be further subdivided into low Fe–Ti and high Fe–Ti subtypes, but the limited number of samples currently available negates such further subdivision.

## RARE-EARTH ELEMENT GEOCHEMISTRY

Lithogeochemical results from analyses of the dykes are plotted on REE and multi-element plots normalized to chondrite (CN) and primitive mantle (PM), respectively (Figure 5). Type-1, -4, and -5 have elevated average $(La/Yb)_{CN}$ ratios of 7.07, 6.91 and 8.18, respectively, significantly higher than the ratios for Type-2 and -3 dykes (3.59 and 3.21, respectively; Table 1). Type-1 dykes have the most prominent negative Nb anomalies, as indicated by their comparatively high $(Th/Nb)_{CN}$ and $(La/Nb)_{CN}$ ratios (Table 1). Type-1 samples also have the most pronounced, albeit small, negative Eu anomalies (mean Eu/Eu* = 0.88; Table

**Table 2.** Selected representative lithogeochemical data for intrusive rocks from the Bonavista Peninsula. All oxides are in wt. % whereas trace elements are given in ppm. UTM coordinates are in NAD27, Zone 22. Key: $FeO^T$ – total iron as ferrous iron; < – concentration is below the given detection limit; N/A – not analyzed; Mg# – [molecular $MgO/(MgO+FeO^T)]*100$

| Sample | D.L. | 13AM152B01 | 13AM280B01 | 15AM141 | 14AM286A01 | 13AM057C01 | 13AM279A01 |
|---|---|---|---|---|---|---|---|
| Easting | | 303987.86 | 303795.91 | 326789.66 | 314727 | 303596.54 | 304389.86 |
| Northing | | 5367266.06 | 5379241.79 | 5360035.33 | 5346683 | 5358325.88 | 5354980.96 |
| Crosscuts | | CPG | CPG | Big Head Fm; MG | Rocky Hr Fm; MG | CPG | Manuels Fm; MG |
| Type | | 1 | 2 | 3 | 4 | 5 | 5 |
| SiO2 | 0.01 | 44.29 | 46.89 | 44.14 | 48.15 | 38.19 | 46.49 |
| TiO2 | 0.001 | 0.68 | 2.53 | 3.62 | 3.13 | 1.47 | 1.86 |
| Al2O3 | 0.01 | 11.91 | 15.95 | 13.30 | 14.90 | 12.45 | 15.58 |
| FeOT | | 9.13 | 12.70 | 14.37 | 12.10 | 7.76 | 11.55 |
| Fe2O3T | 0.01 | 10.15 | 14.11 | 15.97 | 13.45 | 8.62 | 12.84 |
| Fe2O3 | 0.01 | 1.56 | 3.06 | 5.09 | 3.96 | 1.40 | 1.86 |
| FeO | 0.01 | 7.73 | 9.95 | 9.79 | 8.54 | 6.50 | 9.88 |
| MnO | 0.001 | 0.220 | 0.280 | 0.381 | 0.306 | 0.290 | 0.240 |
| MgO | 0.01 | 13.80 | 4.50 | 5.02 | 4.40 | 6.28 | 6.13 |
| CaO | 0.01 | 9.08 | 4.27 | 5.93 | 6.47 | 13.04 | 7.92 |
| Na2O | 0.01 | 1.80 | 4.70 | 3.31 | 3.66 | 1.91 | 3.16 |
| K2O | 0.01 | 0.49 | 1.05 | 0.36 | 2.14 | 1.46 | 0.31 |
| P2O5 | 0.001 | 0.110 | 0.680 | 0.571 | 1.186 | 0.270 | 0.300 |
| Cr | 1 | 834 | 1 | 48 | n/a | 317 | 166 |
| Zr | 1 | 40 | 270 | 256 | 397 | 158 | 112 |
| Ba | 1 | 456 | 460 | 109 | 655 | 322 | 367 |
| LOI | 0.01 | 5.52 | 3.38 | 5.98 | 2.59 | 15.08 | 3.65 |
| Total | | 98.06 | 98.33 | 98.57 | 100.37 | 99.06 | 98.49 |
| Mg# | | 72.92 | 38.69 | 38.35 | 39.34 | 59.06 | 48.62 |
| V | 5 | 294 | 162 | 464 | 135 | 238 | 288 |
| Co | 1 | 58 | 28 | 22 | 21 | 41 | 43 |
| Ga | 1 | 15 | 22 | 24 | 24 | 16 | 24 |
| Ge | 1 | 2.0 | 4.0 | 7.8 | 6.0 | 3.0 | 3.0 |
| As | 5 | n/a | n/a | 11 | 4 | n/a | 6 |
| Sr | 1 | 175 | 248 | 96 | 299 | 626 | 480 |
| Y | 1 | 10 | 39 | 63 | 55 | 19 | 22 |
| Nb | 1 | 3.8 | 14.4 | 14.4 | 45.8 | 23.5 | 20.3 |
| Mo | 2 | 2 | n/a | 2.0 | 2.0 | 2.0 | 2.0 |
| Cd | 0.2 | n/a | n/a | n/a | n/a | n/a | 0.2 |
| Li | 1 | 64.6 | 35.7 | 74.6 | 36.8 | 79.2 | 90.8 |
| Sn | 1 | 1 | 2 | 3 | 3 | 1 | 2 |
| Cs | 0.5 | 0.9 | n/a | 0.7 | 0.6 | n/a | n/a |
| Be | 0.1 | 0.6 | 1.6 | 2.4 | 2.6 | 3.7 | 0.9 |
| Cu | 1 | 97 | 21 | 1 | 12 | 58 | 54 |
| Mn | 1 | 1521 | 1917 | 2640 | 2096 | 1989 | 1621 |
| Ni | 1 | 126 | 14 | 14 | 13 | 146 | 57 |
| Pb | <1 | n/a | n/a | n/a | n/a | n/a | n/a |
| Rb | 1 | 8 | 35 | 17 | 39 | 54 | 10 |
| Sc | 0.1 | 52 | 26.5 | 46.9 | 24.5 | 25.5 | 29.9 |
| Ti | 1 | 4232 | 15800 | 21723 | 18959 | 8893 | 11466 |
| Zn | 1 | 66 | 120 | 145 | 139 | 78 | 102 |
| La | 0.5 | 9.7 | 26.5 | 20.0 | 49.6 | 22.7 | 16.9 |
| Ce | 0.5 | 20.1 | 60.9 | 52.0 | 113.9 | 49.0 | 32.1 |
| Pr | 0.1 | 2.60 | 8.40 | 7.50 | 14.80 | 6.20 | 4.20 |
| Nd | 0.2 | 11.6 | 39.3 | 35.9 | 64.8 | 25.1 | 18.4 |
| Sm | 0.1 | 2.7 | 9.0 | 9.8 | 14.6 | 4.8 | 4.5 |
| Eu | 0.1 | 0.75 | 2.72 | 3.10 | 4.40 | 1.41 | 1.65 |
| Tb | 0.1 | 0.4 | 1.3 | 2.0 | 2.0 | 0.7 | 0.8 |
| Gd | 0.1 | 2.6 | 9.3 | 12.3 | 13.5 | 4.6 | 4.8 |
| Dy | 0.1 | 2.3 | 8.1 | 12.5 | 11.4 | 3.7 | 4.6 |
| Ho | 0.1 | 0.4 | 1.5 | 2.6 | 2.2 | 0.7 | 0.9 |
| Er | 0.1 | 1.1 | 4.6 | 7.5 | 6.1 | 1.9 | 2.3 |
| Tm | 0.1 | 0.15 | 0.59 | 1.07 | 0.79 | 0.25 | 0.33 |
| Yb | 0.1 | 1.0 | 3.9 | 6.8 | 5.1 | 1.5 | 2.2 |
| Lu | 0.1 | 0.16 | 0.60 | 1.11 | 0.76 | 0.23 | 0.31 |
| Hf | 0.2 | 1.4 | 6.2 | 7.4 | 9.6 | 4.3 | 2.9 |
| Ta | 0.5 | n/a | 1.2 | 1.1 | 3.3 | 2.0 | 1.8 |
| W | 1 | 1 | n/a | 4 | n/a | n/a | 1 |
| Tl | 0.1 | n/a | n/a | n/a | n/a | n/a | n/a |
| Bi | 0.4 | 0.5 | n/a | n/a | n/a | n/a | n/a |
| Th | 0.1 | 3.0 | 1.4 | 2.0 | 3.6 | 3.1 | 2.0 |
| U | 0.1 | 0.9 | 0.4 | 0.6 | 1.1 | 1.2 | 0.6 |

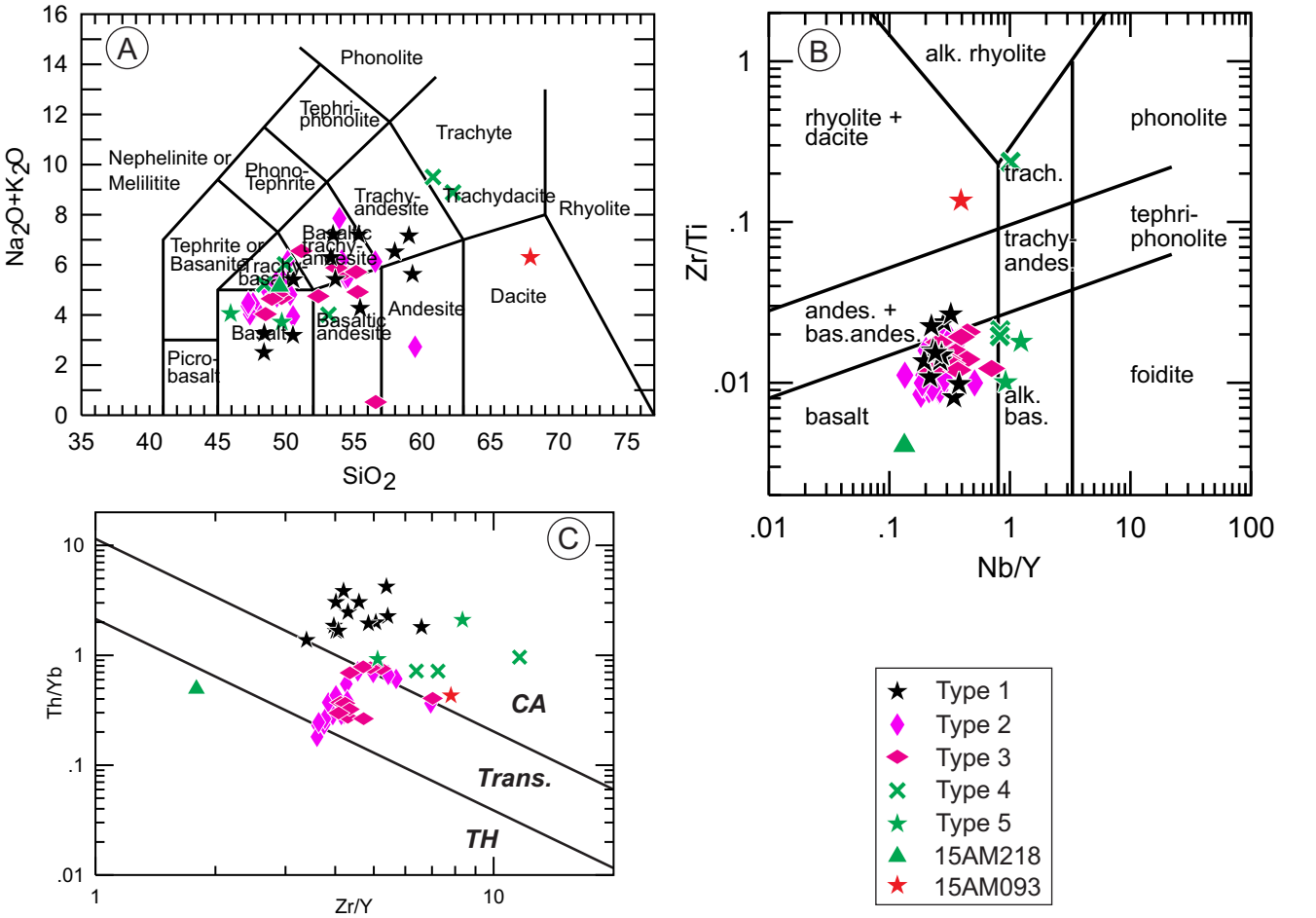


**Figure 2.** *Lithogeochemical classification of mafic intrusive rocks from the Bonavista Peninsula. A) Total alkalis* vs. *silica diagram (LeBas* et al.*, 1986); B) Zr/Ti* vs. *Nb/Y rock classification diagram (Pearce, 1996); C) Th/Yb* vs. *Zr/Y discrimination diagram (Ross and Bédard, 2009) showing tholeiitic (TH), transitional (Trans) and calc-alkaline (CA) fields. Symbols (lower right) apply to all lithogeochemistry diagrams.*

1). Most Type-1 dykes also exhibit negative Zr–Hf and Ti anomalies (Figure 5B).

Relative to Type-1, Type-2 dykes display less fractionated REE patterns (Figure 5C), with $(La/Yb)_{CN}$ ranging from 2.41 to 5.29 (mean of 3.59; Table 1). Most Type-2 dykes have weak HFSE troughs, with the exception of P, which is undepleted to slightly enriched, and many Type-2 dykes lack a negative Ti anomaly. The most primitive Type-2 dykes (lowest REE abundances) have $TiO_2$ contents between 1.50 and 1.75 wt. %, whereas all others have relatively high $TiO_2$ contents (2.33–3.68 wt. % $TiO_2$). Of the high $TiO_2$ variety, three also have high P, indicating accumulation of apatite. These dykes do not exhibit Eu anomalies (mean Eu/Eu* = 1.00).

Type-3 dykes have the least fractionated REE and extended REE patterns of all dyke types (Figure 5E, F), as evident by their low $(La/Yb)_{CN}$, $(La/Sm)_{CN}$, and $(Gd/Yb)_{CN}$ ratios (Table 1). They are distinguishable from Type-2 dykes by their weak (to absent) negative Nb anomalies, as indicated by their relatively low $(La/Nb)_{CN}$ and $(Th/Nb)_{CN}$ ratios (Table 1). They also have less pronounced Zr–Hf troughs than the Type-2 dykes.

Type-4 dykes have some notable variations: two samples show pronounced negative P and Ti anomalies and have elevated Zr–Hf (Figure 5I, J). These plot as trachytes (Figure 2A) and may represent evolved fractionates of this group. Two dykes have slightly positive P spikes and variably negative Ti troughs, and one has very modest Ti and P troughs. Relative to the other types, Type-4 dykes have the lowest Ni and V abundances and the lowest $(Th/Nb)_{CN}$.

Type-5 dykes have the most relative LREE enrichment, and therefore the highest $(La/Yb)_{CN}$, $(La/Sm)_{CN}$, and

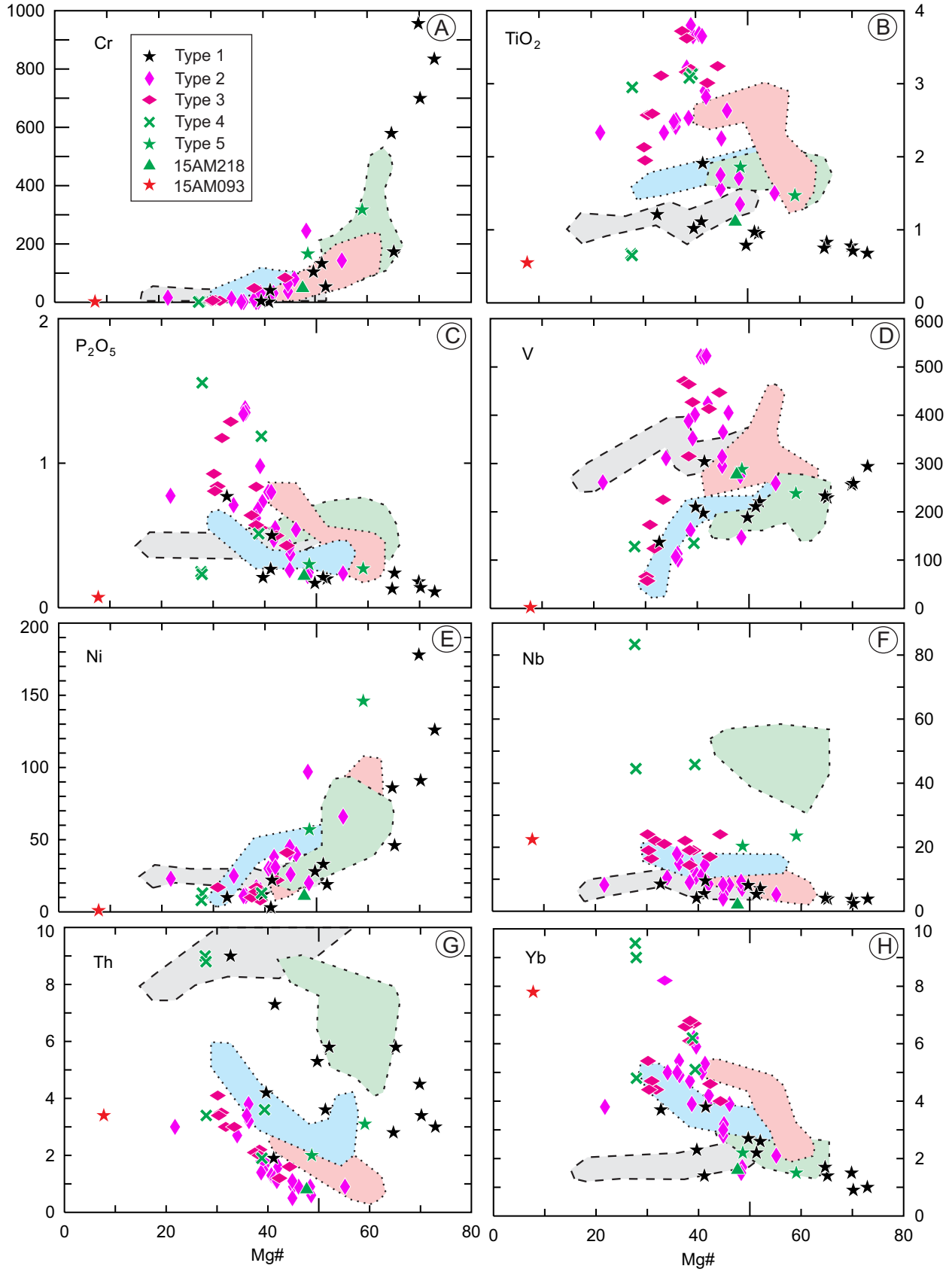


**Figure 3.** *Caption* see *page 31.*

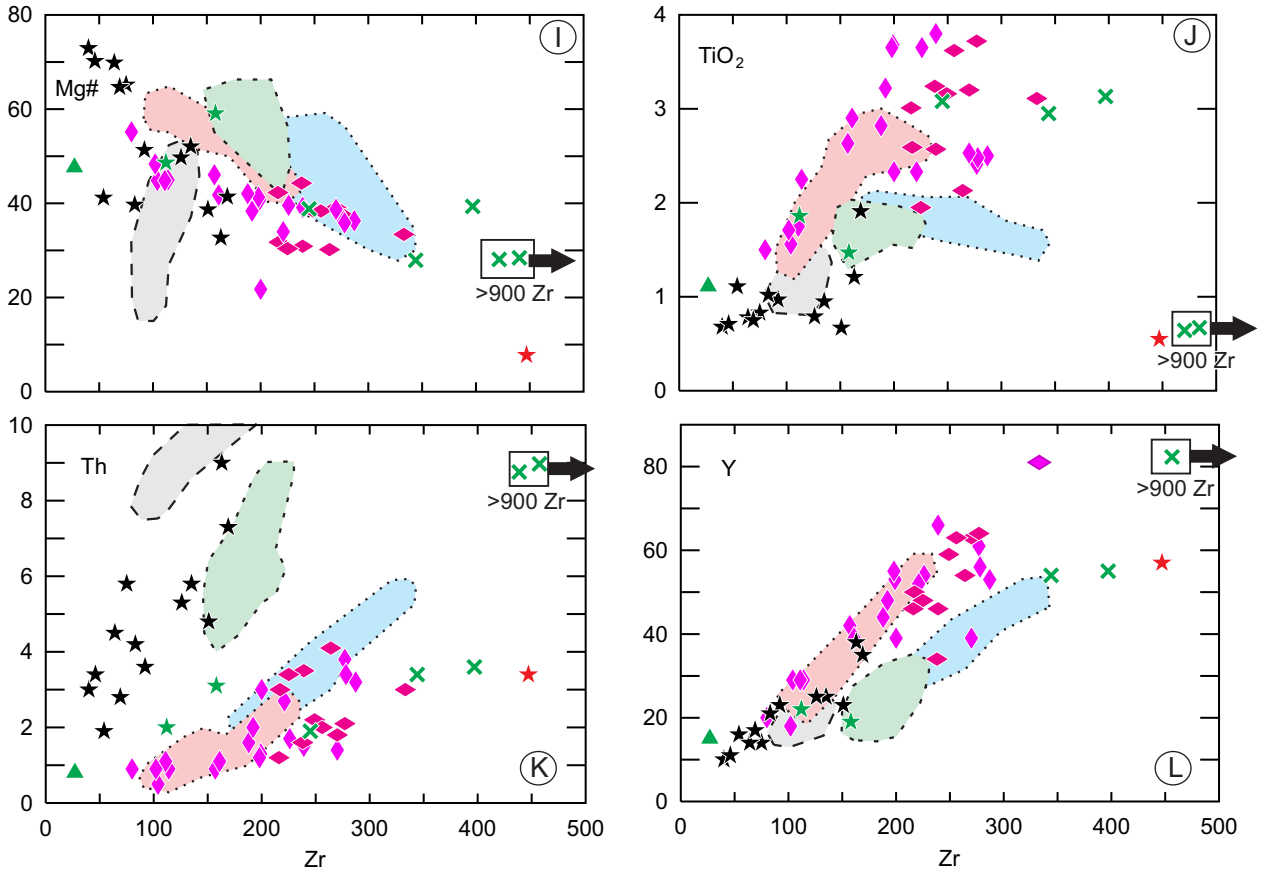


**Figure 3.** *Selected bivariate diagrams. A) Cr* vs. *Mg#; B) $TiO_2$* vs. *Mg#; C) $P_2O_5$* vs. *Mg#; D) V* vs. *Mg#; E) Ni* vs. *Mg#; F) Nb* vs. *Mg#; G) Th* vs. *Mg#; H) Yb* vs. *Mg#; I) Mg#* vs. *Zr; J) $TiO_2$* vs. *Zr; K) Th* vs. *Zr; L) Y* vs. *Zr. Mg# – [MgO/(MgO+FeO$^T$)]*100; Coloured polygons represent fields for volcanic rocks from the Bonavista area: grey – HB; blue – PCvb1; pink – PCvb2; green – DP (from Mills and Sandeman, 2015).*

$(Gd/Yb)_{CN}$ ratios of all dyke types. They lack Nb anomalies and therefore have the lowest $(La/Nb)_{CN}$ ratios. Type-5 dykes also lack Eu anomalies.

Two dykes do not fit into the five petrochemical subdivisions established here. Both dykes are located in the Sweet Bay area and crosscut CPG rocks on the northwestern part of the Bonavista Peninsula. Both dykes show moderate relative LREE enrichment (Figure 5K). Sample 15AM093 is considerably more enriched in REEs than sample 15AM218, and has deep P and Ti troughs, consistent with removal of apatite and titanite, respectively. Sample 15AM218 exhibits Nb, Zr and Hf troughs and a small positive P spike (Figure 5L). Both outliers have a slightly concave-upward pattern in HREEs.

## DIFFERENCES IN DYKE TYPES AND PRELIMINARY PETROGENETIC CONSTRAINTS

Based on petrographic and geochemical evaluation, mafic dykes of the Bonavista Peninsula are divided into five distinct types (Figures 4–6), with two petrological outliers. Most of the mafic dykes, with the exception of some of the Type-1 dykes and one Type-5 dyke (Sample 13AM057C01), have moderate to low Mg#'s, Cr and Ni contents (Figure 3). Hence, these dykes do not represent primary melts of a depleted asthenospheric mantle, but have likely undergone various degrees of fractionation during ascent. The most primitive of the Type-1 dykes have Mg#'s, Cr and Ni abundances that are compatible with derivation from undepleted asthenospheric mantle (*e.g.*, Roeder and Emslie, 1970; Ringwood, 1975).

Continental arc affinity is indicated for nearly all the Bonavista dykes in the Zr/Y *vs.* Zr plot (Pearce, 1983; Figure 4E), except for a single outlier (sample 15AM218). The calc-alkaline Type-1 dykes are LREE-enriched, have negative HFSE anomalies and high Th/Nb ratios, consistent with formation in a subduction zone setting (Pearce, 1996 and references therein). On the Pearce (2008) Ti–Yb proxy for melting depth diagram, Type-1 dyke samples define a vertical, curvilinear array (Figure 6A), consistent with magmatic

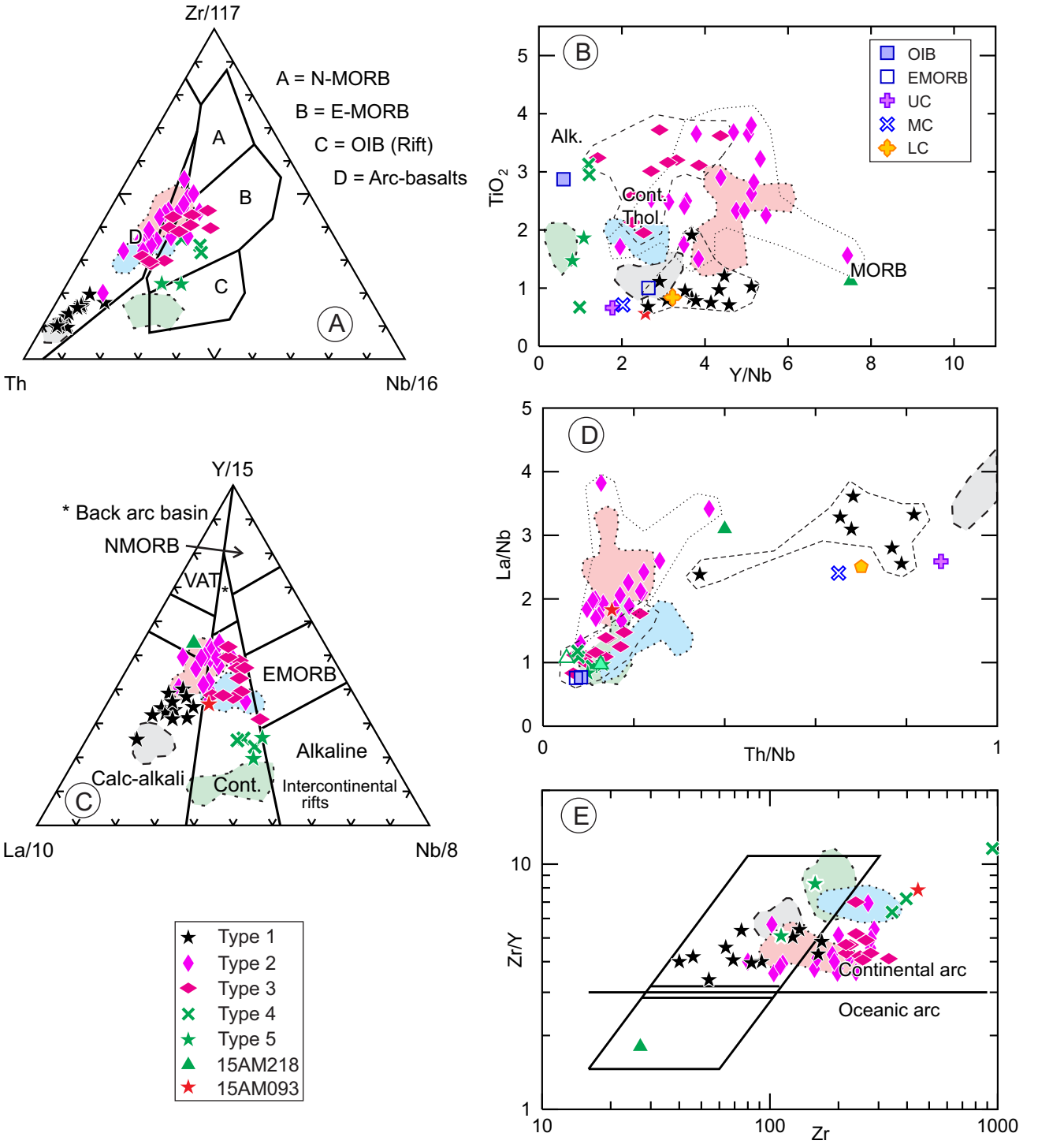


**Figure 4.** *Geochemical data for Bonavista mafic intrusive rocks plotted on selected discrimination diagrams. A) Th–Nb–Zr discrimination plot (Wood, 1980); B) $TiO_2$* vs. *Y/Nb, showing approximate fields for alkaline, continental tholeiite and MORB (Floyd and Winchester, 1975); C) La–Y–Nb tectonic discrimination diagram (Cabanis and Lecolle, 1989); D) La/Nb* vs. *Th/Nb; E) Zr/Y* vs. *Zr discrimination plot (Pearce, 1983) showing fields for continental arc and oceanic arc. Key to dyke types shown on lower left; volcanic fields as per Figure 3; dashed or dotted fields are added for Type-1, Type-2 and Type-3 dykes where visually beneficial; OIB – average ocean-island basalt; E-MORB – enriched mid-ocean-ridge basalt (from Sun and McDonough, 1989); UC – average upper crust; MC – average middle crust; LC – average lower crust (from Rudnick and Gao, 2003).*

evolution *via* fractional crystallization of clinopyroxene and plagioclase from an enriched, shallow asthenospheric source. Type-1 dykes also have the highest Th/Yb ratios of all dykes, indicative of significant lithospheric recycling processes during formation (Figure 6B). These incompatible element relationships suggest that the LILE-enriched Type-1 dykes were erupted in a mature, continental subduction setting (Pearce, 1982, 2008). Despite the small size of the field for HB (Figure 6) owing to the small sample population (n=5), minor overlap is evident between the Type-1 dykes and HB, suggesting a possible petrogenetic link.

Type-2 and -3 dykes are petrochemically similar and have compositions comparable to continental tholeiites (Winchester and Floyd, 1977; Thompson *et al.*, 1983), based on their high $TiO_2$ content relative to calc-alkaline basalts, and high Y/Nb relative to alkaline basalts (Figure 4B). Type-2 dykes can be distinguished from Type-3 dykes by the more pronounced Nb troughs, and higher La/Nb, Th/Nb, and Y/Nb ratios of the former (Table 2 and Figure 4B, D). Type-3 dykes also lack the Zr–Hf troughs exhibited by most Type-2 dykes. On the Pearce (2008) $TiO_2$/Yb *vs.* Nb/Yb diagram (Figure 6A), Type-2 and -3 dykes plot within the enriched part of the MORB array, with the former clustering at slightly lower Nb/Yb ratios, and the Type-3 dykes predominantly clustering at slightly higher Nb/Yb ratios compared to the Type-1 dykes. Type-2 dykes commonly overlap with the field defined by PCvb Series 2, closer to N-MORB, whereas Type-3 dykes plot close to the PCvb Series 1 field (Figure 6A). Type-2 and -3 dykes show similar chemical signatures, indicative of crustal contamination in terms of their variable, but elevated, Th/Yb ratios (Figure 6B). But, the two define different evolutionary trends reflected by their somewhat differing Nb/Yb ratios (Figure 6A, B), indicating that they are not co-magmatic. However, Type-2 and -3 dykes may be petrogenetically related to PCvb2 and PCvb1, respectively, as indicated by their partially overlapping fields (Figures 4B–D and 6A).

Type-4 and -5 dykes are the most fractionated rocks and are alkalic, with both types plotting in the E-MORB field in Figure 6A, owing to their high Nb/Yb ratios. Type-5 dykes plot just above the shallow-melting asthenospheric array of Pearce (2008; E-MORB field on Figure 6A), indicating that, relative to the other dyke types, they more closely approach OIB-like compositions and may have originated from a lower degree of melting at greater depths, likely with minor residual garnet. Although the Type-5 dykes plot proximal to the MORB–OIB array, minor lithospheric contamination is inferred from their high Th/Yb ratios (Figure 6B). Neither the Type-4 nor -5 dykes are interpreted to be petrogenetically linked to the HB, PCvb or DP volcanic units of Mills and Sandeman (2015), although one sample of a Type-5 dyke (sample 13AM057C) plots very close to the DP field in both the Pearce (2008) proxy for melting depth and the proxy for crustal input (Figure 6A, B, respectively).

## GEOCHRONOLOGICAL CONSTRAINTS

New geochronological data (Mills *et al.*, 2016b; Mills *et al.*, *this volume*) from igneous rocks of the Bonavista Peninsula, coupled with lithogeochemistry of the volcanic rocks (Mills and Sandeman, 2015) and biostratigraphy, help to constrain the timing of emplacement of the five dyke-sets described above. Type-1 dykes are geochemically most similar to the HB in terms of their petrochemistry (Figures 4–6), and the dykes may possibly represent feeders to these flows. The best age estimate for the HB flows is *ca.* 600 ± 3 Ma, based on the age of a crystal tuff exposed ~1 m below a HB flow (Mills *et al.*, 2016b).

Type-2 dykes exhibit transitional, arc-like to E-MORB-like characteristics that, relative to the volcanic suites investigated previously (Mills and Sandeman, 2015), are most similar to the Series 2 basaltic flows in the PCvb2 (Figures 4A–D and 6A, B). Although no age constraint has been directly determined for the basaltic rocks in the PCvb, two tuffaceous rocks from the west and east margin of the belt yielded ages of 592 ± 2.2 Ma and 591 ± 1.6 Ma, respectively (Mills *et al.*, *this volume*), and basalt flows most proximal to (above and below) the former are part of the PCvb2 series. Despite no clear intersection of the Type-1 and -2 dykes observed in the field, we infer that the Type-2 dykes are younger than the HB and the Type-1 dykes, based on petrochemical similarity between Type-1 dykes and HB, and Type-2 dykes and basalts of the PCvb2. Whereas it is premature to interpret Type-1 and -2 dykes as feeders to *ca.* 600 Ma HB and *ca.* 592 Ma PCvb2 mafic volcanism, respectively, the dykes reflect a change from arc to continental tholeiite magmatism that is similar to the magmatic shift indicated by the petrochemistry of the volcanic rocks.

Type-3 dykes are petrochemically most similar to basaltic flows of the PCvb1 (Figures 4 and 6), despite the small sample population (n=4) defining fields for the PCvb1 on all discrimination diagrams. These dykes are presumed to be younger than Type-2 based on observed crosscutting relations of the Type-3 dykes with the MG, compounded by the absence of Type-2 dykes within the MG. Further, Type-3 dykes crosscut grey siltstone that is interpreted to overlie the 579 Ma glaciomarine, Gaskiers-equivalent, Trinity facies (Normore, 2010, 2011; Pu *et al.*, 2016). The petrochemical similarities between Type-2 dykes and PCvb2 and, albeit more tenuously, between Type-3 dykes and PCvb1 further imply that PCvb1 basalts are younger than PCvb2 basalts [*i.e.*, series nomenclature of Mills and Sandeman (2015) preceded geochronological constraints]. These data are consistent with a temporal transition from Type-2 dyke–PCvb2

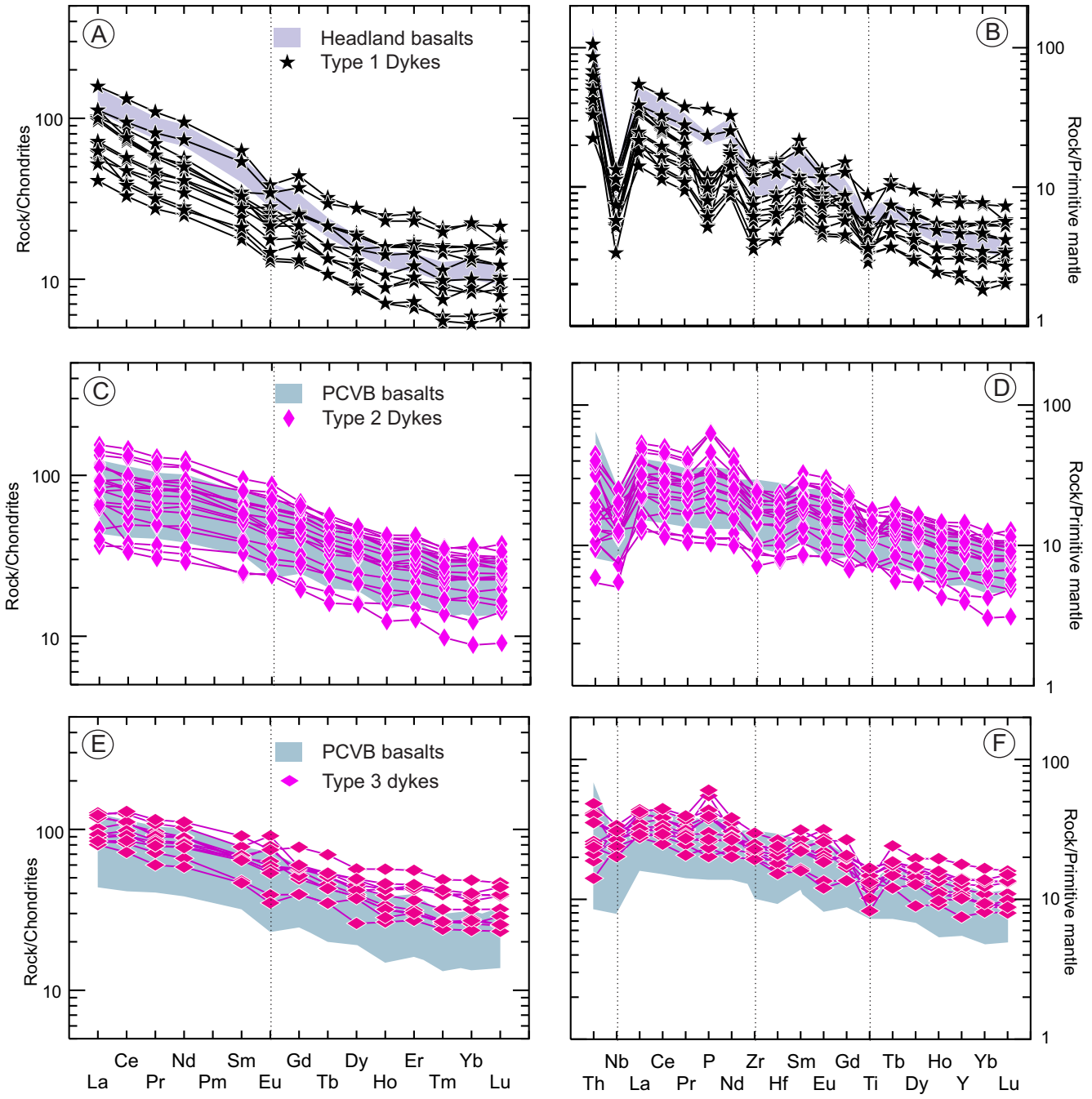


**Figure 5.** *Chondrite-normalized REE and primitive-mantle-normalized multi-element patterns for mafic intrusive rocks of the Bonavista Peninsula (normalizing values from Sun and McDonough, 1989).*

magmas toward the Type-3–PCvb1 magmas, with the latter derived from more enriched mantle source at similarly shallow asthenospheric depth relative to the former. These magmas may all be products of arc extension, having 'continental tholeiitic' character.

A Type-5 dyke crosscuts black shale of the Manuels Formation, Harcourt Group, at Ocean Pond (Mills, 2014). Fragments of trilobite fossils identified as *Paradoxides davidis* and *Jincella* sp. indicate the black shale is Drumian (Cambrian, 504.5–500.5 Ma; *see* Mills, 2014). The margins of the north-northeast-trending dyke were not observed in the field. However, because the dyke is undeformed and cuts Cambrian rocks that are tightly folded, it may be younger than the Acadian (Devonian) deformation that produced the prominent north-northeast-trending cleavage within the Adeyton and Harcourt groups.

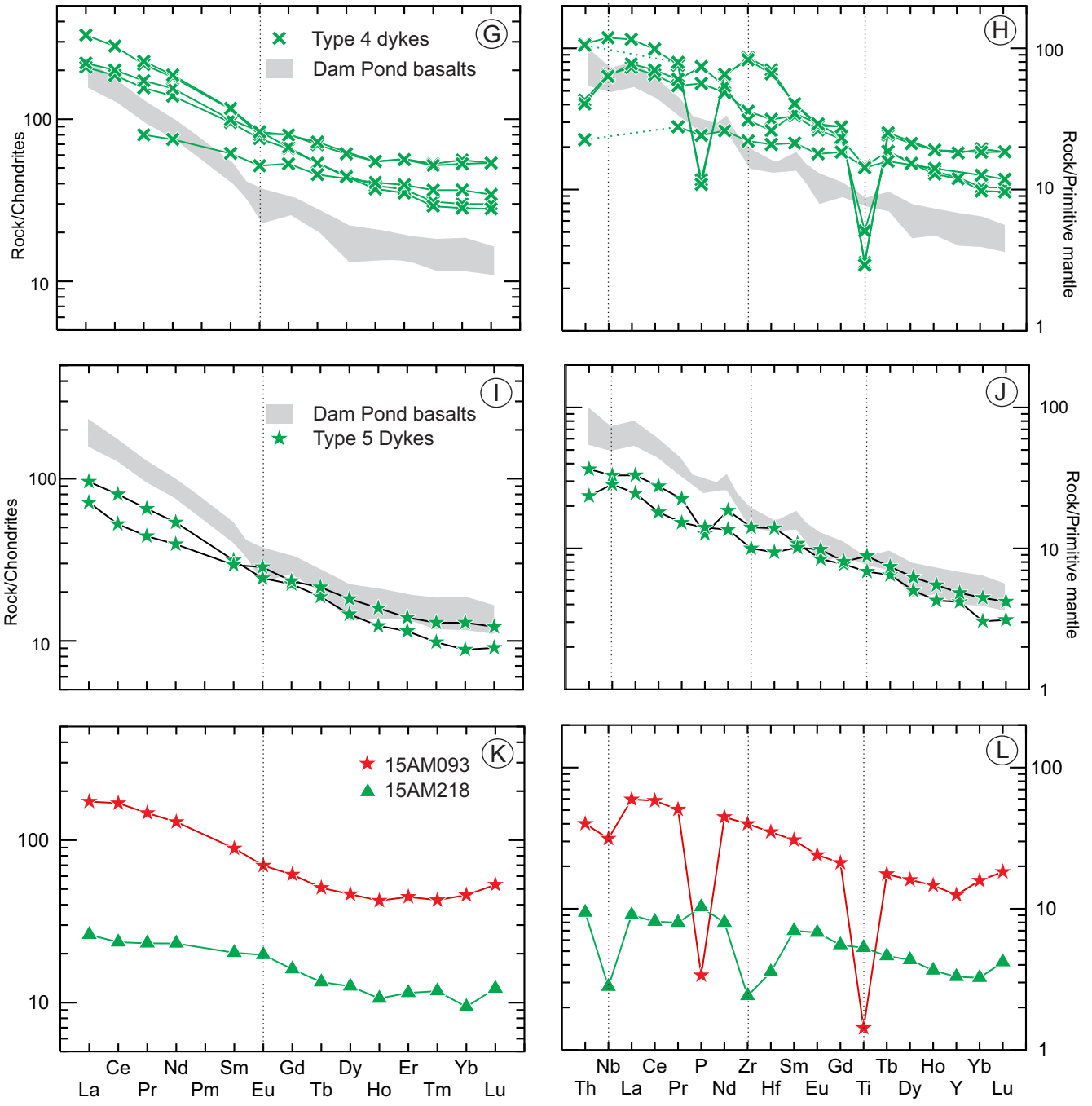


**Figure 5.** *Continued.*

No direct geochronological constraints can currently be applied to Type-4 dykes. These occur in the vicinity of British Harbour, to the southeast of the PCvb. However, given the emerging picture of changing arc-like to tholeiitic (E-MORB) magmatism in the Precambrian, followed by alkalic magmatism in the Paleozoic, it is proposed that the Type-4 dykes and related flows in the British Harbour area are likely younger than Type-1, -2 and -3, but older than the Cambrian (or younger) Type-5 dykes.

## DISCUSSION AND TECTONIC IMPLICATIONS

Field, petrographic and lithogeochemical observations provide new data on the nature and setting of five distinct sets of mafic dykes on the Bonavista Peninsula. The presence of coarse, honeycombed and sieve-textured plagioclase phenocrysts in many of the dykes indicates a complex petrogenetic history involving repetitive replenishment of

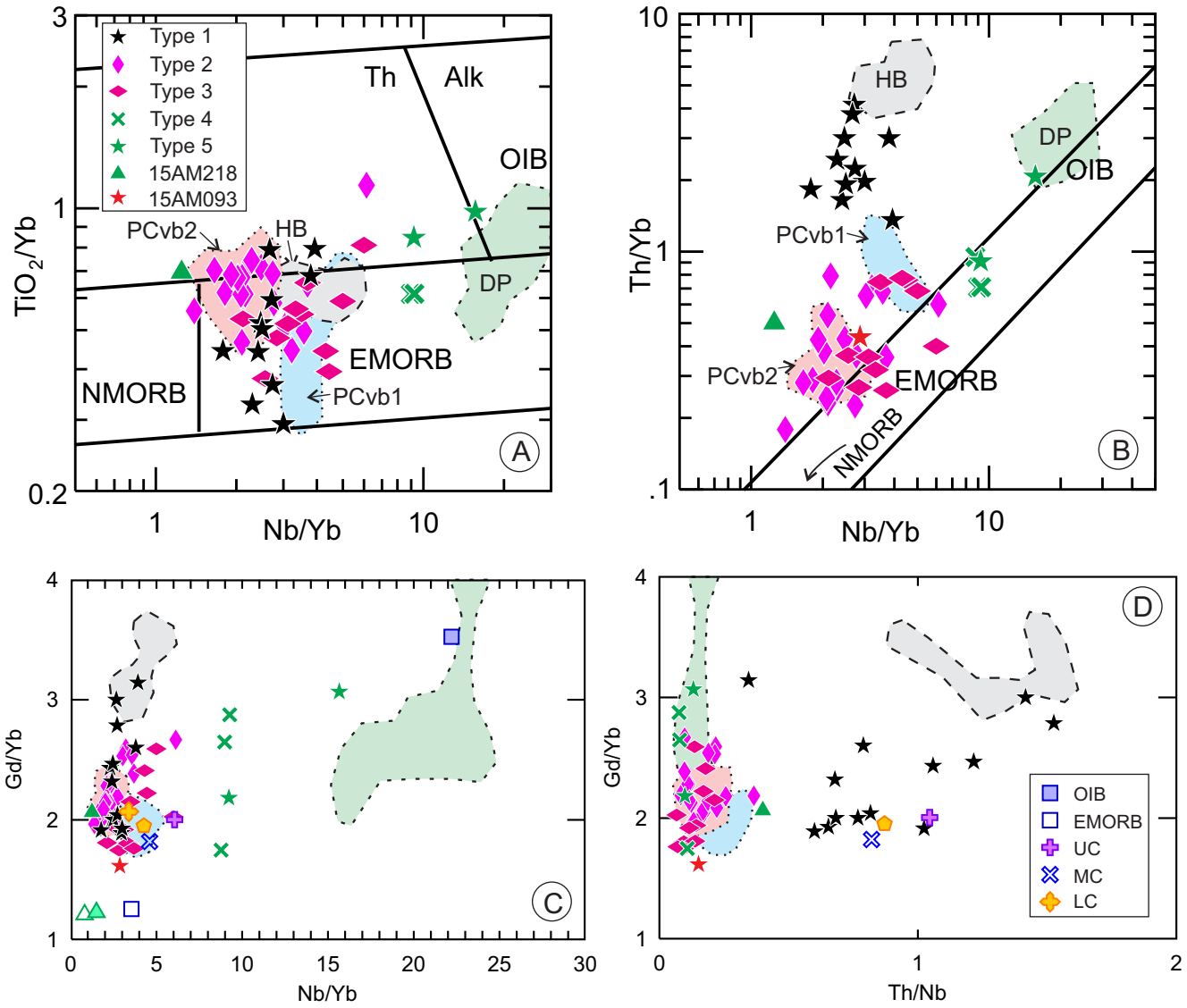


**Figure 6.** *Mafic intrusive rocks of the Bonavista Peninsula (key to dyke types as per Figure 2; volcanic fields as per Figure 3) plotted on selected ratio-ratio diagrams. A) Melting depth proxy, $TiO_2$/Yb vs, Nb/Yb (after Pearce, 2008); B) Crustal input proxy, Th/Yb* vs. *Nb/Yb (after Pearce, 2008); C) Gd/Yb* vs. *Nb/Yb; D) Gd/Yb* vs. *Th/Nb. Key: OIB – average ocean-island basalt; E-MORB – enriched mid-ocean-ridge basalt (Sun and McDonough, 1989); UC – average upper crust; MC – average middle crust; LC – average lower crust (from Rudnick and Gao, 2003).*

magma chambers and recycling of antecrysts from earlier magmas. Type-1 dykes are LILE- and LREE-enriched basalts having deep HFSE troughs, and are likely related to *ca.* 600 Ma volcanic-arc basalts that erupted in a mature continental subduction setting. Type-2 and -3 dykes are considered to represent *ca.* 592 Ma and, possibly <579 Ma continental tholeiites or arc-rift basalts that likely erupted in response to trans-tensional movements along the margin of the PCvb (Mills *et al.*, *this volume*). The alkalic Type-4 dykes are apparently spatially restricted, within-plate, basalts. Type-5 dykes show no significant depletion in HFSE (Figure 5), but are LREE- and LILE-enriched, have a within-plate signature, and likely formed as low degree partial melts of relatively deep, enriched mantle.

Petrological examination of intrusive and extrusive rocks that form the BAF of the Bonavista Peninsula allow for correlation with rocks from parts of the Avalon Terrane outside of Newfoundland. Calc-alkaline, porphyritic basalts of the 613 ± 5 Ma Keppoch Formation, Georgeville Group, Antigonish Highlands of northern mainland Nova Scotia (Murphy *et al.*, 1990, 1992), are similar to Type-1 dykes and HB magmatism in the Bonavista area. In Nova Scotia, the calc-alkaline basaltic flows are interfingered with aphyric,

Fe- and Ti-enriched flows derived from an E-MORB source. The latter are interpreted as continental tholeiites (Murphy *et al.*, 1990), similar to Type-2 dykes–PCvb2 magmatism. Rocks of similar age and petrogenesis are also documented in the Jeffers Group of the Cobequid Highlands (Pe-Piper and Murphy, 1992). In both the Antigonish and Cobequid highlands of Nova Scotia, rocks characterized as continental tholeiites are interpreted as the magmatic products of trans-tensional strike–slip faulting along a basin developed on the margin of a continental arc (Murphy *et al.*, 1990). Similarly, in Massachusetts, deposition of the <595 Ma Roxbury conglomerate of the Boston Bay Group is interpreted to result from syn-depositional extension of the 609 to 584 Ma Dedham–Lynn–Mattapan–Brighton arc assemblage (Thompson *et al.*, 2014). The new geochronological constraints on the timing of volcanism in the PCvb (Mills *et al.*, *this volume*), together with structural and stratigraphic interpretations, indicate that rocks of the PCvb and overlying conglomerate were similarly deposited in a *ca.* 592 Ma trans-tensional setting. These presently disparate parts of the Avalon Terrane, including the Bonavista Peninsula, record evidence of *ca.* 592 Ma extension, commonly associated with transitional, weakly calc-alkaline to E-MORB-like magmatism, of a slightly older 620–600 Ma continental arc terrane.

## REFERENCES


Cabanis, B. and Lecolle, M.
1989: Le diagramme La/10-Y/15-Nb/8: un outil pour la discrimination des series volcaniques et la mise en evidence des processus de mélange et/ou de contamination crustale. Comptes Rendus de l'Acadamie des Sciences, Series II, Volume 309, pages 2023-2029.

Dec, T., O'Brien, S.J. and Knight, I.
1992: Late Precambrian volcaniclastic deposits of the Avalonian Eastport basin (Newfoundland Appalachians): Petrofacies, detrital clinopyroxene and paleotectonic implications. Precambrian Research, Volume 59, pages 243-262.

Finch, C.J.
1998: Inductively coupled plasma-emission spectrometry (ICP-ES) at the Geochemical Laboratory. *In* Current Research. Government of Newfoundland and Labrador, Department of Mines and Energy, Geological Survey, Report 98-1, pages 179-193.

Floyd, P.A. and Winchester, J.A.
1975: Magma type and tectonic setting discrimination using immobile elements. Earth and Planetary Science Letters, Volume 27, pages 211-218.

Hayes, A.O.
1948: Geology of the area between Bonavista and Trinity bays, eastern Newfoundland. Geological Survey of Newfoundland, Bulletin 32 (Part 1), pages 1-37.

Hussey, E.M.
1979: The stratigraphy, structure and petrochemistry of the Clode Sound map area, northwestern Avalon Zone, Newfoundland. Unpublished M.Sc. thesis, Memorial University of Newfoundland, 312 pages.

Jenness, S.E
1963: Terra Nova and Bonavista map-areas, Newfoundland (2D E ½ and 2C). Geological Survey of Canada, Memoir 327, 184 pages.

Knight, I. and O'Brien, S.J.
1988: Stratigraphy and sedimentology of the Connecting Point Group and related rocks, Bonavista Bay, Newfoundland: an example of a Late Precambrian Avalonian basin. *In* Current Research. Government of Newfoundland and Labrador, Department of Mines, Mineral Development Division, Report 88-1, pages 207-228.

Kretz, R.
1983: Symbols for rock-forming minerals. American Mineralogist, Volume 68, pages 277-279.

Lebas, M.J., Lemaitre, R.W., Streckeisen, A. and Zanettin, B.
1986: A chemical classification of volcanic rocks based on the total alkali silica diagram. Journal of Petrology, Volume 27, Number 3, pages 745-750.

Longerich, H.P., Jenner G.A., Fryer, B.J. and Jackson S.E.
1990: Inductively coupled plasma - mass spectrometric analysis of geological samples: a critical evaluation based on case studies. Chemical Geology, Volume 83, pages 105-118.

Malpas, J.G.
1971: The petrochemistry of the Bull Arm Formation near Rantem Station, southeast Newfoundland. Unpublished M.Sc. thesis, Memorial University of Newfoundland, 126 pages.

Middelburg, J.J., Van der Weijden, C.H. and Woittiez, J.R.W.
1988: Chemical processes affecting the mobility of major, minor and trace elements during weathering of granitic rocks. Chemical Geology, Volume 68, pages 253-273.

McCartney, W.D.
1967: Whitbourne map area, Newfoundland. Geological Survey of Canada, Memoir 341, 135 pages.

Mills, A.J.
2014: Preliminary results from bedrock mapping in the Sweet Bay area (parts of NTS map areas 2C/5 and 2C/12), western Bonavista Peninsula, Newfoundland. *In* Current Research. Government of Newfoundland and Labrador, Department of Natural Resources, Geological Survey, Report 14-1, pages 135-154.

Mills, A.J., Calon, T. and Peddle, C.
2016a: Preliminary investigations into the structural geology of the Bonavista Peninsula, northeast Newfoundland. *In* Current Research. Government of Newfoundland and Labrador, Department of Natural Resources, Geological Survey, Report 16-1, pages 133-152.

Mills, A.J., Dunning, G.R., Murphy, M. and Langille, A.
*This volume*: New geochronological constraints on the timing of magmatism for the Bull Arm Formation, Musgravetown Group, Avalon Terrane, northeastern Newfoundland.

Mills, A.J., Dunning, G.R. and Langille, A.
2016b: New geochronological constraints on the Connecting Point Group, Bonavista Peninsula, Avalon Zone, Newfoundland. *In* Current Research. Government of Newfoundland and Labrador, Department of Natural Resources, Geological Survey, Report 16-1, pages 153-171.

Mills, A.J. and Sandeman, H.A.I.
2015: Preliminary lithogeochemistry for mafic volcanic rocks from the Bonavista Peninsula, northeastern Newfoundland. *In* Current Research. Government of Newfoundland and Labrador, Department of Natural Resources, Geological Survey, Report 15-1, pages 173-189.

Murphy, J.B., Keppie, J.D., Dostal, J. and Hynes, A.J.
1990: The geochemistry and petrology of the Late Precambrian Georgeville Group: a volcanic arc rift succession in the Avalon Terrane of Nova Scotia. Geological Society of America, Special Paper 51, pages 383-393.

Murphy, J.B., Keppie, J.D., Dostal, J. and Nance, R.D.
1999: Neoproterozoic–early Paleozoic evolution of Avalonia. *In* Laurentia–Gondwana Connections Before Pangea. *Edited by* V.A. Ramos and J.D. Keppie. Geological Society of America, Special Papers, Volume 336, pages 253-266.

Murphy, J.B., Pe-Piper, G., Keppie, J.D. and Piper, D.J.W.
1992: Correlation of Neoproterozoic III sequences in the Avalon Composite Terrane of mainland Nova Scotia: tectonic implications. Atlantic Geology, Volume 28, pages 143-151.

Normore, L.S.
2010: Geology of the Bonavista map area (NTS 2C/11), Newfoundland. *In* Current Research. Government of Newfoundland and Labrador, Department of Natural Resources, Geological Survey, Report 10-1, pages 281-301.

2011: Preliminary findings on the geology of the Trinity map area (NTS 2C/060, Newfoundland. *In* Current Research. Government of Newfoundland and Labrador, Department of Natural Resources, Geological Survey, Report 11-1, pages 273-293.

O'Brien, S.J., Dunning, G.R., Knight, I. and Dec, T.
1989: Late Precambrian geology of the north shore of Bonavista Bay (Clode Sound to Lockers Bay). *In* Report of Activities. Government of Newfoundland and Labrador, Department of Mines, Geological Survey, pages 49-50.

O'Brien, S.J. and King, A.F.
2002: Neoproterozoic stratigraphy of the Bonavista Peninsula: preliminary results, regional correlations and implications for sediment-hosted stratiform copper exploration in the Newfoundland Avalon Zone. *In* Current Research. Government of Newfoundland and Labrador, Department of Mines and Energy, Geological Survey, Report 02-1, pages 229-244.

2005: Late Neoproterozoic (Ediacaran) stratigraphy of the Avalon Zone sedimentary rocks, Bonavista Peninsula, Newfoundland. *In* Current Research. Government of Newfoundland and Labrador, Department of Natural Resources, Geological Survey, Report 05-1, pages 101-114.

Pearce, J.A.
1982: Trace element characteristics of lavas from destructive plate boundaries. *In* Andesites. *Edited by* R.S. Thorpe. John Wiley and Sons, New York, 724 pages.

1983: Role of the sub-continental lithosphere in magma genesis at active continental margins. *In* Continental Basalts and Mantle Xenoliths. Papers prepared for a UK Volcanic Studies Group meeting at the University of Leicester, pages 230-249.

1996: A user's guide to basalt discrimination diagrams. *In* Trace Element Geochemistry of Volcanic Rocks; Applications for Massive Sulphide Exploration. Short Course Notes, Geological Association of Canada, Volume 12, pages 79-113.

2008: Geochemical fingerprinting of oceanic basalts with applications to ophiolite classification and the search for Archean oceanic crust. Lithos, Volume 100, pages 14-48.

Pe-Piper, G. and Murphy, J.B.
1992: Late Proterozoic high-titanium basalts in the Avalon Zone of Nova Scotia. Canadian Mineralogist, Volume 30, pages 1167-1176.

Pu, J.P., Bowring, S.A., Ramezani, J., Myrow, P., Raub, T.D., Landing, E., Mills, A., Hodgin, E. and Macdonald, F.A.
2016: Dodging snowballs: Geochronology of the Gaskiers glaciation and the first appearance of the Ediacaran biota, Geology, Geological Society of America, Data Repository item 2016326; doi: 10.1130/G38284.1, 4 pages.

Ringwood, A.E.
1975: Composition and petrology of the Earth's mantle. McGraw-Hill Book Co., New York, N.Y., USA, 618 pages.

Roeder, P.L. and Emslie, R.F.
1970: Olivine-liquid equilibrium. Contributions to Mineralogy and Petrology, Volume 29, pages 275-289.

Ross, P.-S. and Bédard, J.H.
2009: Magmatic affinity of modern and ancient subalkaline volcanic rocks determined from trace-element discriminant diagrams. Canadian Journal of Earth Sciences, Volume 46, pages 823-839.

Rudnick, R.L. and Gao, S.
2003: Composition of the continental crust. *In* Treatise on Geochemistry. *Edited by* H.D. Holland and K.K. Turekian. Volume 3, The Crust, Elsevier-Pergamon Press, Oxford, pages 1-64.

Smith, S.A. and Hiscott, R.N.
1984: Latest Precambrian to Early Cambrian basin evolution, Fortune Bay, Newfoundland: fault-bounded basin to platform. Canadian Journal of Earth Sciences, Volume 21, pages 1379-1392.

Sun, S.S. and McDonough, W.F.
1989: Chemical and isotopic systematics of oceanic basalts: implications for mantle composition and processes. *In* Magmatism in the Ocean Basin. *Edited by* A.D. Saunders and M.J. Norry. Geological Society of London, Special Publication 42, pages 313-345.

Taylor, S.R. and McLennan, S.M.
1985: The Continental Crust: Its Composition and Evolution. Blackwell Scientific Publications, Oxford.

Thompson, R.N., Morrison, G.L., Dickin, A.P. and Hendry, G.L.
1983: Continental flood basalts… Arachnids rule OK? *In* Continental Basalts and Mantle Xenoliths. *Edited by* C.J. Hawkesworth and M.J. Norry. Shiva Geology Series, pages 158-185.

Thompson, M.D., Ramezani, J. and Crowley, J.L.
2014: U-Pb zircon geochronology of Roxbury Conglomerate, Boston Basin, Massachusetts: Tectonostratigraphic implications for Avalonia in and beyond SE New England. American Journal of Science, Volume 314, June 2014, pages 1009-1040.

Widmer, K.
1949: Unpublished map and incomplete report on the Glovertown–Clode Sound area. Geological Survey of Newfoundland [2D/9/65].

Winchester, J.A. and Floyd, P.A.
1977: Geochemical discrimination of different magma series and their differentiation products using immobile elements. Chemical Geology, Volume 20, pages 325-343.

Wood, D.A.
1980: The application of a Th-Hf-Ta diagram to problems of tectomagmatic classification and to establishing the nature of crustal contamination of basaltic lavas of the British Tertiary Volcanic Province. Earth and Planetary Science Letters, Volume 50, pages 11-30.